Response to Comments by Referee #1

Thank you for your commendation and appreciate your suggestions on all scientific, technical aspects of our article. The manuscript has been revised accordingly. Listed below is our point-to-point response to each comment.

General comments:

This paper reports a comparison of primary emissions and secondary organic aerosol formation from one gasoline direct injection (GDI) and one port fuel injection (PFI) gasoline vehicle. There is a limited but nonetheless useful study and interpretation of the formation of secondary organic aerosol (SOA) in relation to the low molecular weight aromatic compounds contained within the exhaust. My main concern over this paper is that previous work has shown quite substantial variations between vehicles of similar engine specification using the same fuel, and hence comparing one GDI vehicle with one PFI vehicle and then making very general statements about one technology versus another has the potential to mislead seriously. In this context, the title of the paper is most inappropriate as there is no evidence that the vehicles tested are representative of GDI and PFI vehicles more generally. For this reason, major modifications are recommended and the overall tenor of the paper needs to be much more subdued in relation to the comparison.

Response: We thank the referee for pointing out this. The gasoline vehicles tested in this study are representative in market share in China. And we agree with the referee that one vehicle for each gasoline engine technology exists uncertainty. We will conduct more experiments with more vehicles. We have revised title and added discussions as the suggestion.
The title is revised as: "Comparison of primary aerosol emission and secondary aerosol formation from gasoline direct injection and port fuel injection vehicles".
Following discussions are added between Line 312 to Line 315: "It should be pointed out that the SOA formation factors in this study are based on one GDI vehicle and one PFI vehicle. Some previous studies proposed that vehicles have variations even though they meet similar specification vehicles and use the same fuel (Gordon et al., 2014; Jathar et al., 2014). Thus more researches with more vehicles for each technology are needed on SOA formation from vehicle exhaust".

There are also issues over the way in which the technologies are described. Lines 25-26 state that "these studies show that GDI vehicles emit more primary particles than PFI vehicles, and even diesel vehicles equipped with diesel particulate filter" and lines 289-290 state that "the considerable particle number emitted by gasoline vehicles, especially in GDI vehicles exhaust... needs to be controlled in the future emissions standards". This ignores the fact that the European Euro 6 regulations set a particle mass and a number emissions standard for GDI which is the same as the emissions standard for diesel vehicles and consequently GDI engines with high particle emissions are fitted with particulate filters in order to meet the emissions regulations. Such filters will remove elemental carbon and POA as well as reducing the emission of organic vapors (as they have catalytic

activity), and consequently SOA production will be substantially reduced. Thus, the GDI vehicle tested in this study is almost certainly not representative of current GDI vehicles on sale in Europe (and most probably North America, although I am less familiar with that market) and for this reason also, the presentation of the results is likely to prove highly misleading.

Response: Thanks for the suggestion. In China, the PN will be restricted in China Phase VI Emissions Standard in 2020, so the gasoline particulate filters (GPFs) have not been used widely. The gasoline vehicles certified China Phase IV and V Emissions Standard dominate current on-road gasoline vehicles. Thus, this study could reflect the gasoline vehicle emissions in China and other developing countries. Moreover, it should be acknowledged that the GPFs have significant contribution on reducing primary aerosol emission from GDI vehicles (Chan et al., 2014). Some studies also reported that the VOCs emission from GDI vehicles might be reduced by catalyzed GPFs (Ito et al., 2015), which would lead to SOA formation reduction. Therefore, further studies on GPFs are needed in our future studies.

Specific comments:

Other points worthy of attention are the following: (a) Line 71 states that the gasoline fuel meets the China phase V fuel standard. This means nothing to the general reader. Fuel quality standards have in recent years been driven by sulphur content. As a minimum, the sulphur content of this fuel should be indicated.

Response: Thanks for your suggestion. Accepted, and adding sulfur content of the fuel between Line 88 to Line 90: "The fuel used in the experiments was a typical Phase V gasoline on the China market (sulfur content = 6 mg kg^{-1}). More information of the fuel is provided in Table S1 in the Supplement".

Table S1 Details of the fuel used in the experiments.

Specifications	Fuel
Density (g mL^{-1})	0.7
Rvp (kPa)	55.4
Aromatics (% v/v)	36.7
Olefin (% v/v)	15.4
Ethanol (% v/v)	0.01
Oxygen (% m/m)	0.02
Mn (mg kg^{-1})	< 0.1
Sulfur (mg kg^{-1})	6
T10 (℃)	55.4
T50 (℃)	109.9
T90 (℃)	164.3
Fbp (℃)	194.4

(b) Line 240-241 suggests that since semi-volatile vapours may partition more strongly into the particle phase at higher aerosol concentrations, this would increase SOA formation. There are two factors here. The authors appear to be referring to the partitioning of the oxidation products which will give an increase in SOA yield at higher pre-existing particle loadings. However, there is a second effect which may be more significant. If the precursors of the SOA partition more strongly into the condensed phase at higher ambient particle loadings, there will be less vapour phase compound present to be oxidised and therefore the rate of SOA production will be reduced. This point needs to be considered when discussing the SOA yields on page 9.

Response: Thanks for your suggestion. The two aspects are considered and added between Line 248 to Line 256:
"Although particle wall-loss correction as well as particle and gas dilution corrections were considered in this study, several factors may still contribute to the uncertainties of the SOA productions. First, the deposition of semi-volatile vapors to the chamber walls was not corrected, which may result in an underestimation of the rate of SOA production with a factor of 1.1-4.1 (Zhang et al., 2014). Second, under some ambient conditions such as severe urban haze events (Guo et al., 2014), particle mass concentrations can be as high as 200-300 $\mu g\ m^{-3}$, much higher than the 23 ± 6 $\mu g\ m^{-3}$ under the chamber condition in this study. High particle mass loadings are favorable for the partition of semi-volatile compounds into the particle phase, potentially increasing the rate of SOA production (Odum et al., 1996). Third, stronger partitioning of SOA precursors into the particle phase may reduce the oxidized products in the gas phase, which will potentially reduce the rate of SOA production (Seinfeld et al., 2003)".

(c) Table 2 refers to measurement of OC/EC but does not specify the analyser or the protocol. This should be included.

Response: We thank the reviewer for reminding this. The instrument for OC/EC measurement is added between Line 126 to Line 128: "...to analyze the mass, organic carbon (OC) and elemental carbon (EC) emission factors using a balance and OC/EC analyzer (Sunset Lab, USA)".

(d) Table 4 reports emission factors for PAH but does not specify which compounds.

Response: Thanks for the suggestions. The PAHs emission factor reported in this study is a sum of 31 polycyclic aromatic hydrocarbons compounds. Their emission factors are listed in the Table S2 in the Supplement.

Table S2 The EFs of Particulate-phase PAHs from GDI and PFI vehicles.

Compound	Emission factor (ng km^{-1})	
	GDI	PFI
Napthalene	0.025	<0.0001
1-Methylnaphthalene	<0.0001	<0.0001
2-Methylnaphthalene	0.012	0.004
2,6-Dimethylnaphthalene	0.006	0.003
Acenaphthylene	0.012	0.009
Acenapthene	<0.0001	0.015
Fluorene	0.003	0.105
Methyl-fluorene	0.083	0.105
Dibenzofuran	0.006	0.039
Retene	0.009	0.011
9-Methylanthracene	<0.0001	0.013
Phenanthrene	0.244	0.069
Anthracene	0.048	0.018
Fluoranthene	0.201	0.034
Pyrene	0.246	0.029
Methyl-fluoranthene	0.004	0.007
Benzo[a]anthracene	0.006	0.036
Chrysene	0.020	0.065
Methyl-chrysene	<0.0001	0.007
Benzo[b]fluoranthene	0.034	0.147
Benzo[k]fluoranthene	0.041	0.129
Benzo[e]pyrene	0.028	0.051
Benzo[a]pyrene	0.012	0.041
Benzo[ghi]flouranthene	0.095	0.027
Cyclopenta[cd]pyrene	<0.0001	0.032
Dibenzo[a,h]anthracene	<0.0001	<0.0001
Picene	<0.0001	<0.0001
Perylene	0.009	<0.0001
Benzo[ghi]perylene	<0.0001	<0.0001
Indeno[1,2,3-cd]pyrene	<0.0001	<0.0001
Coronene	<0.0001	<0.0001
Sum PAHs	1.144	0.994

Reference

Chan, T. W., Meloche, E., Kubsh, J., and Brezny, R.: Black Carbon Emissions in Gasoline Exhaust and a Reduction Alternative with a Gasoline Particulate Filter, Environmental science & technology, 48, 6027-6034, 10.1021/es501791b, 2014.

Guo, S., Hu, M., Zamora, M. L., Peng, J., Shang, D., Zheng, J., Du, Z., Wu, Z., Shao, M., Zeng, L., Molina, M. J., and Zhang, R.: Elucidating severe urban haze formation in China, Proceedings of the National Academy of Sciences of the United States of America, 111, 17373-17378, 10.1073/pnas.1419604111, 2014.

Ito, Y., Shimoda, T., Aoki, T., Yuuki, K., Sakamoto, H., Kato, K., Their, D., Kattouah, P., Ohara, E. and Vogt, C.: Next Generation of Ceramic Wall Flow Gasoline Particulate Filter with Integrated Three Way Catalyst, SAE Technical Paper 2015-01-1073, 2015, doi:10.4271/2015-01-1073, 2015.

Gordon, T. D., Presto, A. A., May, A. A., Nguyen, N. T., Lipsky, E. M., Donahue, N. M., Gutierrez, A., Zhang, M., Maddox, C., Rieger, P., Chattopadhyay, S., Maldonado, H., Maricq, M. M., and Robinson, A. L.: Secondary organic aerosol formation exceeds primary particulate matter emissions for light-duty gasoline vehicles, Atmos. Chem. Phys. , 14, 4661-4678, 10.5194/acp-14-4661-2014, 2014.

Jathar, S. H., Gordon, T. D., Hennigan, C. J., Pye, H. O. T., Pouliot, G., Adams, P. J., Donahue, N. M., and Robinson, A. L.: Unspeciated organic emissions from combustion sources and their influence on the secondary organic aerosol budget in the United States, Proc. Natl. Acad. Sci. USA, 111, 10473-10478, 10.1073/pnas.1323740111, 2014.

Odum, J. R., Hoffmann, T., Bowman, F., Collins, D., Flagan, R. C., and Seinfeld, J. H.: Gas/particle partitioning and secondary organic aerosol yields, Environ. Sci. Technol., 30, 2580-2585, 10.1021/es950943+, 1996.

Seinfeld, J. H., Kleindienst, T. E., Edney, E. O., and Cohen, J. B.: Aerosol growth in a steady-state, continuous flow chamber: Application to studies of secondary aerosol formation, Aerosol Science and Technology, 37, 728-734, 10.1080/02786820390214954, 2003.

Zhang, X., Cappa, C. D., Jathar, S. H., McVay, R. C., Ensberg, J. J., Kleeman, M. J., and Seinfeld, J. H.: Influence of vapor wall loss in laboratory chambers on yields of secondary organic aerosol, Proc. Natl. Acad. Sci. USA, 111, 5802-5807, 10.1073/pnas.1404727111, 2014.

1 **Comparison of primary aerosol emission and secondary aerosol formation from gasoline direct injection and**

2 **port fuel injection vehicles**

3 Zhuofei Du[1], Min Hu[1, 3*], Jianfei Peng[1†], Wenbin Zhang[2], Jing Zheng[1], Fangting Gu[1], Yanhong Qin[1], Yudong Yang[1],

4 Mengren Li[1], Yusheng Wu[1], Min Shao[1], Shijin Shuai[2]

5 1. State Key Joint Laboratory of Environmental Simulation and Pollution Control, College of Environmental

6   Sciences and Engineering, Peking University, Beijing 100871, China

7 2. State Key Laboratory of Automotive Safety and Energy, Department of Automotive Engineering, Tsinghua

8   University, Beijing 100084, China

9 3. Beijing Innovation Center for Engineering Sciences and Advanced Technology, Peking University, Beijing

10   100871, China

11 [†] Now at Department of Atmospheric Sciences, Texas A&M University, College Station, TX 77843, US

12

13 *Corresponding author: Min Hu, minhu@pku.edu.cn

14

15

16 **Abstract**

17 Gasoline vehicles greatly contribute to urban particulate matter (PM) pollution. Gasoline direct injection (GDI)

18 engines, known as their higher fuel efficiency than that of port fuel injection (PFI) engines, have been increasingly

19 employed in new gasoline vehicles. However, the impact of this trend on air quality is still poorly understood. Here,

20 we investigated both primary emissions and secondary organic aerosol (SOA) formation from GDI and PFI vehicles

21 under urban-like condition, using combined approaches involving chassis dynamometer measurement and

22 environmental chamber simulation. The PFI vehicle emits slightly more volatile organic compounds, e.g., benzene

23 and toluene, whereas the GDI vehicle emits more particulate components, e.g., the total PM, elemental carbon,

24 primary organic aerosols and polycyclic aromatic hydrocarbons. Strikingly, a much higher SOA production (by a

25 factor of approximately 2.7) is found from the exhaust of the GDI vehicle than that of the PFI vehicle under the

same conditions. More importantly, the higher SOA production found in the GDI vehicle exhaust occurs concurrently with lower concentrations of traditional SOA precursors, e.g., benzene and toluene, indicating a greater contribution of intermediate volatility organic compounds and semivolatile organic compounds in the GDI vehicle exhaust to the SOA formation. Our results highlight the considerable potential contribution of GDI vehicles to urban air pollution in the future.

1 Introduction

Organic aerosols account for approximately 20-50 % of ambient fine particulate matter ($PM_{2.5}$), with significant environment and health effects (Kanakidou et al., 2005). Primary organic aerosol (POA) is emitted directly by sources, while secondary organic aerosol (SOA) is mainly formed via oxidation of gaseous precursors in the atmosphere and account for about 30-90 % of the organic aerosol (OA) mass worldwide (Zhang et al., 2007; Hu et al., 2016), but SOA source remain poorly constrained. Robinson et al. (2007) proposed that low-volatility gas-phase species emitted from diesel vehicles were important sources for urban ambient SOA, which achieved better mass closure between observed and modeled SOA. Using an updated CMAQ model, Jathar et al. (2017) found that 30-40% OA was contributed from vehicles in the southern California, and half of which was SOA. Huang et al. (2014) recently revealed that 15-65 % of SOA was contributed by fossil fuel consumption (i.e., traffic and coal burning) in megacities in China. These indicated that vehicles have important contribution to ambient SOA in urban areas. An ambient organic aerosol measurement in the Los Angeles Basin demonstrated that SOA contributed from gasoline vehicles was significant in the urban air, much larger than that from diesel vehicles (Bahreini et al., 2012). Similar conclusion was reached by Hayes et al. (2013) based on mass spectrometer results. Meanwhile, several chamber simulation studies concluded that exhaust of gasoline vehicles could form substantial SOA (Jathar et al., 2014). Thus, gasoline vehicles exhaust is highly associated with ambient SOA formation.

Gasoline vehicles can be categorized into two types based on the fuel injection technologies in their engines, i.e., port fuel injection (PFI) vehicles and gasoline direct injection (GDI) vehicles. Unlike a PFI engine, in which

gasoline is injected into intake port, gasoline is sprayed into cylinder directly in a GDI engine. With the increased atomization and vaporization rate of fuel, and more accurate control of fuel volume and injection time, a GDI engine has many advantages, such as better fuel efficiency, lower CO_2 emissions and less fuel pumping loss (Alkidas, 2007; Myung et al., 2012; Liang et al., 2013). In past decades, PFI vehicles dominated the market share of gasoline cars in the world. However, in recent years, GDI vehicles have been increasingly employed, due to their higher fuel efficiency. The market share of GDI vehicles in sales in 2016 reached about 25 %, 50 % and 60 % in China, the US and Europe, respectively (Wen et al., 2016; Zimmerman et al., 2016).

Several previous studies investigated the emissions of GDI and PFI vehicles, in terms of concentrations of gaseous pollutants, particle numbers and mass concentrations, and evaluated the reduction of emissions with the upgrading emission standards (Ueberall et al., 2015; Zhu et al., 2016; Saliba et al., 2017). These studies show that GDI vehicles emit more primary particles than PFI vehicles (Zhu et al., 2016; Saliba et al., 2017), and even diesel vehicles equipped with diesel particulate filter (DPF) (Wang et al., 2016), which is likely due to insufficient time allowed for gasoline fuel to be mixed with air thoroughly, as well as gasoline droplets impinging onto pistons and surfaces of combustion chamber in GDI engine (Chen et al., 2017; Fu et al., 2017). However, in most studies, vehicles were tested under the driving cycles of the US or European standards, indicating that those results are not representative of China's traffic conditions.

SOA production from gasoline vehicle exhaust was previously simulated in smog chambers and potential aerosol mass (PAM) flow reactors. SOA formed from gaseous pollutants exceeds the related POA emissions and having much more contribution to air quality degradation. These studies mostly focused on the impacts of SOA formation by the model year (Gordon et al., 2014; Jathar et al., 2014; Liu et al., 2015), fuel formulations (Peng et al., 2017), driving cycles (including idling) (Nordin et al., 2013; Platt et al., 2013) and start-up modes of the gasoline vehicles (Nordin et al., 2013). Few studies, however, have investigated SOA formation from vehicles with different engine technologies (GDI and PFI) under the same working condition.

In this study, both primary emissions and secondary aerosol formation from GDI and PFI vehicles were investigated. To represent typical urban driving patterns in megacities such as Beijing, the vehicles were tested

3

76   using gasoline fuel meeting the China Phase V fuel standard, and were operated with the cold-start Beijing cycle

77   (BJC). The SOA formation from both the PFI and GDI vehicle exhausts were then simulated using a smog chamber.

78   Finally, the overall contributions of the GDI and PFI gasoline vehicles to ambient particulate matter (PM) were

79   evaluated. This study is part of a project that investigates the relationship between vehicle (engine) emissions and

80   ambient aerosols, including potential of SOA formation from a PFI engine (Du et al., 2017) and the effects of

81   gasoline aromatics on SOA formation (Peng et al., 2017).

82

2 Materials and methods

2.1 Vehicles

85   One PFI vehicle and one GDI vehicle were tested in this study to investigate their primary emissions and SOA

86   formations. In this study, the selected PFI and GDI vehicles were certified to the China Phase IV Emissions

87   Standard (equivalent to Euro IV) and the China Phase V Emissions Standard (equivalent to Euro V), respectively.

88   More information of the vehicles is shown in Table 1. The fuel used in the experiments was a typical Phase V

89   gasoline on the China market (sulfur content = 6 mg kg^{-1}). More information of the fuel is provided in Table S1 in

90   the Supplement. Cold-start BJC, characterized by a higher proportion of idling periods and lower acceleration

91   speeds than the New European Driving Cycle (NEDC), was performed to simulate the repeated braking and

92   acceleration on road in megacities such as Beijing. The BJC lasted approximately 17 minutes, with a maximum

93   speed of 50 km h^{-1} (Peng et al., 2017).

94

2.2 Experimental setup

96   The chamber experiments were carried out in the summer at the State Key Laboratory of Automotive Safety

97   and Energy of Tsinghua University in Beijing, including two experiments conducted with GDI vehicle and four

98   experiments conducted with PFI vehicle. The tested vehicles were placed on a chassis dynamometer system (Burke

99   E. Porter Machinery Company) with a controlled room temperature and absolute humidity of 26.4±2.5 ℃ and

100   11.5±2.4 g m^{-3}, respectively. The exhaust emitted by the vehicle tailpipe was diluted in a constant volume sampler

101 (CVS) system, where the flow was maintained at 5.5 m^3 min^{-1} using filtered ambient air, achieving about 20 times

102 dilution of the exhaust. Several instruments, including an AVL CEBII gas analyzer, a Cambustion Differential

103 Mobility Spectrometer (DMS500) and a particle sampler, were connected to the CVS (detailed in Figure 1 and

104 section 2.3) to characterize the primary gas- and particulate-phase pollutants. The diluted exhausts produced by the

105 CVS system were injected into an outdoor chamber, where secondary aerosol formation from gasoline vehicle

106 exhausts was simulated. This was the second dilution step of the exhausts and had a dilution factor of approximately

107 15. A schematic illustration of the outdoor experimental setup is shown in Figure 1.

108 The photochemical oxidation experiments were carried out in a quasi-atmospheric aerosol evolution study

109 (QUALITY) outdoor chamber. More details of the setup and performance of the QUALITY chamber were

110 introduced by Peng et al. (2017). Prior to each experiment, the chamber was covered with a double-layer anti-

111 ultraviolet (anti-UV) shade to block sunlight and was cleaned with zero air for about 15 h to create a clean

112 environment. Approximately 120 ppb O_3 were injected into the chamber prior to the injection of vehicle exhaust to

113 make the oxidation environment similar to the mean O_3 peak concentration in the ambient atmosphere. Before the

114 chamber was exposed to sunlight, about 15-minute period was left to ensure that the pollutants mixed sufficiently

115 in the chamber, then the initial concentrations were characterized in the dark. Subsequently, the anti-UV shade

116 were removed from the chamber and photo-oxidation was initiated. A suite of high time resolution instruments was

117 utilized to track the evolution of pollutants during the chamber experiments. Zero air was added into the chamber

118 when sampling to maintain a constant pressure.

119

120 **2.3 Instrumentation**

121 Primary gases and aerosols were measured by the instruments connected to the CVS. The concentrations of

122 gaseous pollutants, including CO, CO_2, NO_x and total hydrocarbon (THC) were monitored with a gas analyzer

123 AVL Combustion Emissions Bench II (CEB II, AVL, Austria). Primary aerosols were measured with both on-line

124 and off-line instruments. A DMS500 (Cambustion, UK) was implemented to monitor the real-time number size

125 distribution and total number concentration of primary particles. Its sampling line was heated to maintain the

126 temperature at 150℃. The aerosols were also collected on Teflon and quartz filters by AVL Particulate Sampling

127 System (SPC472, AVL, Austria) to analyze the mass, organic carbon (OC) and elemental carbon (EC) emission

128 factors using a balance and OC/EC analyzer (Sunset Lab, USA).

129 During the chamber experiments, a suite of real-time instruments was utilized to characterize the evolutions

130 of the gas and particulate-phase pollutants. CO analyzer, NO-NO_2-NO_x analyzer and O_3 analyzer (Thermo Fisher

131 Scientific Inc., USA) were employed to measure the concentrations of CO, NO_x (including NO and NO_2) and O_3,

132 respectively. The evolutions of volatile organic compounds (VOCs) were monitored with a proton transfer reaction

133 mass spectrometer (PTR-MS, IoniconAnalytik, Austria) (Lindinger et al., 1998). H_3O^+ was used as the reagent ion,

134 which reacted with the target compounds. The resulting ions were detected by a quadruple mass spectrometer.

135 Meanwhile, the particles size distribution was characterized using a scanning mobility particle sizer system (SMPS,

136 TSI, USA), which consisted of a differential mobility analyzer (DMA, TSI, USA) and a condensation particle

137 counter (CPC, TSI, USA). This system can measure aerosols with a diameters ranging from 15 nm to 700 nm. A

138 high-resolution time-of-flight aerosol mass spectrometer (HR-Tof-AMS, Aerodyne Research, USA) was applied to

139 obtain mass concentrations and size distributions of submicron, non-refractory aerosols, including sulfate, nitrate,

140 ammonium, chloride and organic (DeCarlo et al., 2006). Table 2 lists the instruments used to measure the primary

141 emissions and their evolutions in the chamber experiments.

142

143 **3 Results**

144 **3.1 Primary emissions**

145 **Gaseous pollutant emissions**

146 Emission factors (EFs) of CO_2, THC, benzene and toluene from the GDI and PFI vehicles are listed in Table

147 3. The EFs of CO_2 and THC are derived from measured concentrations in CVS, while the EFs of benzene and

148 toluene were calculated from the initial concentrations in the chamber. The THC emission factor was reported in

149 units of carbon mass, g C kg^{-1}fuel^{-1}.

150 The GDI vehicle emitted less CO_2 and THC than the PFI vehicle due to their different fuel injection strategies

151   and mixing features (Liang et al. 2013; Gao et al., 2015). The EF of THC from the GDI vehicle met the standard

152   of the China Phase V Emission Standard (0.1 g km^{-1}), but that from the PFI vehicle was slightly beyond the standard

153   limit. The PFI vehicle used in this study met lower emission standard (the China Phase IV), which might cause

154   additional THC emission when compared to the China Phase V Emission Standard. In addition, BJC and NEDC

155   were applied in this study and emission standard, respectively. More repeated braking and acceleration in BJC

156   might cause incomplete combustion and consequently higher THC emission from the PFI vehicle in this study. As

157   typical VOC species emitted by vehicles, benzene and toluene were measured in this study. For both vehicles, the

158   EFs of toluene were higher than those of benzene. Consistent with the feature of THC emission, the PFI vehicle

159   emitted more benzene and toluene than the GDI vehicle, and the enhancement of toluene was much larger than that

160   of benzene.

161   The EFs of the gaseous pollutants in this study had similar magnitudes to those in previous studies in which

162   gasoline vehicles met comparable levels of emission standards and were tested under cold-start driving condition,

163   while the results in this study were slightly higher, as shown in Table 3. This difference might be because the

164   California ultralow-emission vehicles (ULEV) (Saliba et al., 2017) and most LEV II vehicles (manufactured in

165   2004 or later) (May et al., 2014) meet the US certification gasoline emission standards for the ULEV category,

166   which has a lower limit of gaseous pollutants than the China Phase V Emission Standard. In addition, the different

167   driving cycles of our study and those other studies (listed in Table 3) might be another explanation for the difference

168   in the EFs of gaseous pollutants.

169   **Primary particle emissions**

170   The EFs of PM, elemental carbon (EC), POA and particulate polycyclic aromatic hydrocarbons (PAHs) are

171   shown in Table 4. The EF of PM$_{2.5}$ from the GDI vehicle was about 1.4 times higher than that of the PFI vehicle.

172   Both vehicles met the China Phase V Emission Standard for PM emission (4.5 mg km^{-1}). The GDI vehicle emitted

173   about 3.3 times more EC and 1.2 times more POA than the PFI vehicle. The primary carbonaceous aerosols

174   (EC+POA) accounted for 85 % and 82 % of the PM in the GDI and PFI vehicles respectively, suggesting that

175   carbonaceous aerosols were the major contributors in the PM from gasoline vehicles, especially for the GDI vehicle.

7

176   PAHs account for a small fraction of particulate organic matter in the atmosphere, but the molecular signature

177   of PAHs can be utilized in source identification of vehicle emissions (Kamal et al., 2015). The GDI vehicle emitted

178   about 1.5 times the PAHs of the PFI vehicle. The EFs of PAH compounds are listed in Table S2 in the Supplement,

179   and details of PAHs measurement was described in Li et al. (2016). It should be noted that the PAHs were tested

180   under warm-start cycles. A higher EF of PAHs would be obtained under cold-start cycle, since the lower

181   temperature led to inefficient catalyst at the beginning of cold-start (Mathis et al., 2005). The main contributors to

182   total PAHs mass emitted from gasoline vehicle exhaust in this study, especially from the GDI vehicle exhaust, was

183   similar with the results reported by previous studies (Schauer et al., 2002; Hays et al., 2013).

184   The lower $PM_{2.5}$ and POA emissions from GDI vehicle were found in previous studies, except that a little

185   higher $PM_{2.5}$ emission from GDI vehicle was illustrated in Saliba's study (Platt et al., 2013; May et al., 2014; Zhu

186   et al., 2016; Saliba et al., 2017). The EC emissions were in the range of those of previous studies but on the lower

187   level. The EF of the POA measured in this study was higher than those of other studies, leading to a higher OC/EC

188   ratio, which could be attributed to the less strict emission standard of our vehicles and the different driving cycles

189   applied in the experiments.

190   The bimodal number size distributions of the primary PM from the vehicles measured by the DMS500 are

191   shown in Figure 2. The particle distributions of the exhausts of the GDI and PFI vehicles illustrated similar patterns,

192   with two peaks located at about 10 nm for nucleation mode and at 60-90 nm for accumulation mode, respectively,

193   which are consistent with the results of previous studies (Maricq et al., 1999; Chen et al., 2017). The particle

194   number size distribution of the exhausts of the GDI vehicle showed a similar pattern to that of the PFI vehicle, with

195   a much higher number concentration that is consistent with the emission of more particle mass.

196

197   **3.2 SOA formation from gasoline vehicle exhaust**

198   The time-resolved concentrations of gases and particles during the chamber experiments are illustrated in

199   Figure 3. Before removing the anti-UV shade, the initial concentrations of NO_x, benzene and toluene from the PFI

200   and GDI vehicles were 80 ppb, 3 ppb, 5 ppb and 100 ppb, 4 ppb, 14 ppb respectively.

201 After the aging experiment started (t=0 in Figure 3), NO was formed from NO_2 photolysis, and then reacted

202 with O_3 to form NO_2. The O_3 concentration increased rapidly to a maximum within 2-3 h and then decreased via

203 reactions and dilution. Benzene and toluene decayed during the aging process at different rates.

204 New particle formation was found inside the chamber 15 minutes after the exhaust was exposed to sunlight,

205 providing substantial seeds for secondary aerosol formation. Significant growths of particles in both size and mass

206 were observed in the chamber, indicating that a large amount of secondary aerosol was formed during the

207 photochemical oxidation. The chemical compositions of the secondary aerosols were measured continuously by

208 HR-Tof-AMS. Organic was the dominant composition of the secondary aerosol, accounting for 88-95 % of the

209 total particle mass inside the chamber (Figure S1), which is consistent with our previous research (Peng et al.,

210 2017). The SOA mass exhibited different growth rate for the two types of vehicles. After a 4 h oxidation in the

211 chamber, the SOA formed from the exhaust of the GDI vehicle was approximately double that of the PFI vehicle.

212 The solar radiation conditions significantly influenced the SOA formation. Thus, OH exposure was used to

213 characterize the photochemical age as a normalization, instead of the experiment time. Two VOC species with

214 noticeable differences in their reaction rate constants with OH radicals could be utilized to calculate the OH

215 exposure ([OH] Δt) based on Equation 1 (for benzene and toluene, as used in this study) (Yuan et al., 2012).

216 $$[OH]\,\Delta t = \frac{1}{k_T - k_B} \times \left(\ln \frac{[T]}{[B]}\bigg|_{t=0} - \ln \frac{[T\}}{[B]} \right) \qquad (1)$$

217 where k_T and k_B are the OH rate constants of benzene (1.2×10^{-12} cm^3 molecule^{-1} s^{-1}) (Yuan et al., 2012) and toluene

218 (5.5×10^{-12} cm^3 molecule^{-1} s^{-1}) (Kramp and Paulson, 1998), respectively. $\frac{[T]}{[B]}\bigg|_{t=0}$ is the concentration ratio of

219 toluene to benzene at the beginning of the aging process, and $\frac{[T]}{[B]}$ is their concentration ratio measured during

220 aging process.

221 The SOA concentrations as a function of OH exposure are illustrated in Figure 4. Wall-loss correction and

222 dilution correction, including both particles and gaseous pollutants, were taken into consideration in the calculation

223 of the SOA mass concentration in the chamber. Detailed descriptions of corrections are given in the Supplement.

224 Assuming the mean OH concentration was 1.6×10^6 molecular cm^{-3} in Beijing (Lu et al., 2013), the whole aging

225 procedure in the chamber experiments was equal to a 6-10 h atmospheric photochemical oxidation. The average

226 SOA concentrations were 9.25 ± 1.80 and 4.68 ± 1.32 μg m^{-3} for the GDI and PFI vehicles, respectively, when the

227 OH exposure was 5×10^6 molecular cm^{-3} h in the chamber. Considering the driving cycle mileage and fuel

228 consumption, the SOA productions were 54.77 ± 10.70 mg kg-fuel^{-1} or 3.06 ± 0.60 mg km^{-1} for the GDI vehicle and

229 20.57 ± 5.82 mg kg-fuel^{-1} or 1.55 ± 0.44 mg km^{-1} for the PFI vehicle. Compared with the PFI vehicle, the GDI vehicle

230 exhaust exhibited a higher potential of SOA formation, even though the PFI vehicle emitted more VOCs, which

231 are considered as dominant class of SOA precursors. This result indicates that higher concentrations of some other

232 SOA precursors exist in the exhaust of GDI vehicles, which will be further discussed in section 3.3.

233 The results from chamber simulation of SOA formation from individual gasoline vehicles are illustrated in

234 Figure 5. The SOA production from the both vehicles in this study is in the range of the results of previous studies

235 (Nordin et al., 2013; Platt et al., 2013; Jathar et al., 2014; Liu et al., 2015; Peng et al., 2017). The variation of the

236 SOA production among these studies might be caused by several factors: the model years of vehicles

237 (corresponding to emission standards) (Nordin et al., 2013; Liu et al., 2015), their driving cycles (Nordin et al.,

238 2013), the initial concentrations of gaseous pollutants in the chamber (Jathar et al., 2014), and the ratio of VOCs to

239 NO$_x$ (Zhao et al., 2017) in the chamber experiments.

240 To investigate the dominant contributors to ambient PM from the GDI and PFI vehicles, Figure 6 illustrates

241 the EFs of EC and POA as well as the production factors of SOA in this study. The SOA production from the GDI

242 vehicle was approximately 2.7 times higher than that from the PFI vehicle. At 5×10^6 molecular cm^{-3} h OH exposure,

243 the SOA/POA ratio was approximately 1. Figure 4 illustrates that the SOA production increased with

244 photochemical age rapidly (within 2×10^7 molecular cm^{-3} h). Thus, SOA would exceed POA at higher OH exposure,

245 e.g., the SOA/POA ratio reached about 4 at 10^7 molecular cm^{-3} h OH exposure, becoming the major PM contributor.

246 In terms of the POA and EC emissions as well as the SOA formation, the GDI vehicle contributed 2.2 times more

247 than the PFI vehicle.

248 Although particle wall-loss correction as well as particle and gas dilution corrections were considered in this

249 study, several factors may still contribute to the uncertainties of the SOA productions. First, the deposition of semi-

10

250 volatile vapors to the chamber walls was not corrected, which may result in an underestimation of the rate of SOA

251 production with a factor of 1.1-4.1 (Zhang et al., 2014). Second, under some ambient conditions such as severe

252 urban haze events (Guo et al., 2014), particle mass concentrations can be as high as 200-300 ug m^{-3}, much higher

253 than the 23 $\pm$6 ug m^{-3} under the chamber condition in this study. High particle mass loadings are favorable for the

254 partition of semi-volatile compounds into the particle phase, potentially increasing the rate of SOA production

255 (Odum et al., 1996). Third, stronger partitioning of SOA precursors into the particle phase may reduce the oxidized

256 products in the gas phase, which will potentially reduce the rate of SOA production (Seinfeld et al., 2003)

257

258 **3.3 SOA mass closure**

259 SOA production ($\Delta OA_{predicted}$) estimated from VOC precursors can be defined as Eq. (2):

260 $$\Delta OA_{predicted} = \sum_i (\Delta_i \times Y_i) \qquad (2)$$

261 where Δ_i is the concentration change of precursor VOC$_i$ measured with PTR-MS in the chamber experiments, and

262 Y_i is the SOA yield of the VOC$_i$. In this study, benzene, toluene, C8 benzene and C9 benzene were involved in the

263 estimation of SOA production, and alkanes and alkenes were not considered. A recent study found that ozonolysis

264 of alkenes from gasoline vehicle exhaust could form SOA through aldol condensation reactions (Yang et al., 2018).

265 However, much low declines of concentrations were observed than those of aromatics during chamber experiments,

266 so alkenes might not play significant role in SOA formation in this study.

267 The SOA yield is sensitive to VOCs/NO$_x$ ratio (Song et al., 2005). In this study, the VOCs/NO$_x$ ratio was in

268 the range of 0.5-1.0 ppbC/ppb, thus, the SOA formation from the vehicle exhaust was determined under high NO$_x$

269 conditions. The high NO$_x$ SOA yields of benzene and toluene were taken from Ng et al. (2007). The C8 and C9

270 benzene used the SOA yield of m-xylene from Platt et al. (2013).

271 The increased predicted SOA contribution from the VOC precursors as a function of OH exposure

272 accumulation is demonstrated in Figure 7. At the end of the experiments, the SOA estimated from these speciated

273 VOCs accounted for about 25 % and 53 % of the measured SOA formation from the GDI and PFI vehicle exhausts,

274 respectively. Similar to the results of previous studies (Platt et al., 2013; Nordin et al., 2013; Gordon et al., 2014),

275 single-ring aromatics played an important role in the SOA formation, especially for the PFI vehicle which shows

276 higher predicted SOA fraction.

277 The unpredicted fraction of the measured SOA in the chamber experiments was in the range of 47-75 %.

278 Contributions from intermediate volatility organic compounds (IVOCs) and semivolatile organic compounds

279 (SVOCs), e.g., long branched and cyclic alkanes and gas-phase polycyclic aromatic hydrocarbons could be a

280 possible explanation for this underestimation. The SOA formed by oxidation of IVOCs and SVOCs is found to

281 dominate over that from single-ring aromatics (Robinson et al., 2007; Zhao et al., 2016). The unpredicted SOA

282 ratio exhibited a maximum value at the beginning of the experiment, indicating that the IVOCs and SVOCs with

283 low volatilities produced SOA much more efficiently than the single-ring aromatics with high volatilities, as the

284 first generation products of photo-oxidation of these precursors form SOA (Robinson et al., 2007).

285 The larger fraction of the unpredicted SOA from the GDI vehicle exhaust might be associated with higher

286 IVOCs and SVOCs emissions. Gas-phase PAH is one of the main component of speciated IVOCs (Zhao et al.,

287 2016). The particulate-phase PAHs from the GDI vehicle were more abundant than those from the PFI vehicle by

288 a factor of 1.5 (section 3.1). Based on gas-particle equilibrium, this indicates that more gas-phase PAHs, including

289 some aromatic IVOCs, might be emitted by the GDI vehicles, contributing to the SOA enhancement.

290

4 Discussions and conclusions

292 GDI and PFI vehicles have different fuel injection technologies in their engines, which affects their emissions

293 of gaseous and particulate pollutants. In GDI engine, the fuel is directly injected into cylinder, which benefits the

294 fuel atomization and vaporization and provides better control of fuel volume and the combustion process (Liang et

295 al. 2013; Gao et al., 2015). Thus, in this study, the tested GDI vehicle has higher fuel economy and lower THC

296 emission than the PFI vehicle. However, the insufficient mixing time allowed for the fuel and air leads to

297 incomplete combustion in the GDI engine (Fu et al., 2014). In addition, direct fuel injection leads to fuel

298 impingement onto surfaces of combustion chamber, where liquid pools form, favoring soot-like particulate

299 formation (Ueberall et al., 2015; Chen et al., 2017). Consequently, larger particle mass and number are emitted by

300   the GDI vehicle than from the PFI vehicle. The particles emitted by the GDI vehicle have higher EC mass fraction,

301   leading to lower OC/EC ratio. The considerable particle number emitted by gasoline vehicles, especially in GDI

302   vehicles exhaust, makes a significant contribution to particle number concentration as well as seeds for further

303   reactions in the atmosphere, and needs to be controlled in the future emission standards.

304   Our results show that the GDI vehicle contributes more to both primary and secondary aerosol than the PFI

305   vehicle, and has greater impact on environment and air quality. In recent years, the market share of GDI vehicles

306   exerts a continuous growth in China because they provide better fuel economy and lower CO_2 emissions. In 2016,

307   GDI vehicles accounted for 25 % of China's market share in sales, and this proportion is expected to reach 60 %

308   by 2020 (Wen et al., 2016). The PM enhancement of GDI vehicles with increasing population could potentially

309   offset any PM emission reduction benefits, including the development of gasoline emission and fuel standards and

310   the advanced engine technologies of gasoline vehicles. Therefore, our results highlight the necessity of further

311   research and regulation of GDI vehicles.

312   It should be pointed out that the SOA formation factors in this study are based on one GDI vehicle and one

313   PFI vehicle. Some previous studies proposed that vehicles have variations even though they meet similar

314   specification vehicles and use the same fuel (Gordon et al., 2014; Jathar et al., 2014). Thus more researches with

315   more vehicles for each technology are needed on SOA formation from vehicle exhaust.

316   Primary emissions and secondary organic formation from one GDI vehicle and one PFI vehicle were

317   investigated when driving under cold-start BJC. The primary PM emitted by the GDI vehicle was 1.4 times greater

318   than that from the PFI vehicle and the SOA formation from the GDI vehicle exhaust was 2.7 times greater than that

319   from the PFI vehicle exhaust for the same OH exposure. The SOA production factors were 54.77±10.70 mg kg-

320   fuel^{-1} or 3.06±0.60 mg km^{-1} for the GDI vehicle and 20.57±5.82 mg kg-fuel^{-1} or 1.55±0.44 mg km^{-1} for the PFI

321   vehicle at an OH exposure of 5×10^6 molecular cm^{-3} h, which is consistent with the values seen in previous studies.

322   Considering the higher amounts of OA derived from primary emission and secondary formation, the GDI vehicle

323   contribute considerably more to particle mass concentrations in the ambient air than the PFI vehicle.

324   The SOA formation was predicted from the gaseous precursors emitted by the GDI and PFI vehicles under

325 high NO$_x$ condition. Single-ring aromatic VOCs could explain only 25-53 % of the measured SOA formation in

326 the chamber experiments. The GDI vehicle exhibited higher fraction of unexplained SOA. More IVOCs and

327 SVOCs were inferred as being emitted by the GDI vehicle.

328 With increasing population of GDI vehicles, any benefits of the aerosol emission reduction of gasoline

329 vehicles are substantially offset, because GDI vehicles have significant contributions to ambient aerosols. More

330 work is needed to improve the understanding of GDI vehicle emissions and to provide information for the

331 regulation of gasoline vehicles.

332

333

334 *Data availability*. The data presented in this article are available from the authors upon request

335 (minhu@pku.edu.cn).

336

337

344

345 **Reference**

346 Alkidas, A. C.: Combustion advancements in gasoline engines, Energy Conversion and Management, 48, 2751-

347 2761, 10.1016/j.enconman.2007.07.027, 2007.

348 Bahreini, R., Middlebrook, A. M., de Gouw, J. A., Warneke, C., Trainer, M., Brock, C. A., Stark, H., Brown, S. S.,

349 Dube, W. P., Gilman, J. B., Hall, K., Holloway, J. S., Kuster, W. C., Perring, A. E., Prevot, A. S. H., Schwarz, J. P.,

350 Spackman, J. R., Szidat, S., Wagner, N. L., Weber, R. J., Zotter, P., and Parrish, D. D.: Gasoline emissions dominate

351 over diesel in formation of secondary organic aerosol mass, Geophysical Research Letters, 39,

352 10.1029/2011gl050718, 2012.

353 Chen, L., Liang, Z., Zhang, X., and Shuai, S.: Characterizing particulate matter emissions from GDI and PFI

354 vehicles under transient and cold start conditions, Fuel, 189, 131-140, 10.1016/j.fuel.2016.10.055, 2017.

355 DeCarlo, P. F., Kimmel, J. R., Trimborn, A., Northway, M. J., Jayne, J. T., Aiken, A. C., Gonin, M., Fuhrer, K.,

356 Horvath, T., Docherty, K. S., Worsnop, D. R., and Jimenez, J. L.: Field-deployable, high-resolution, time-of-flight

357 aerosol mass spectrometer, Analytical Chemistry, 78, 8281-8289, 10.1021/ac061249n, 2006.

358 Du, Z., Hu, M., Peng, J., Guo, S., Zheng, R., Zheng, J., Shang, D., Qin, Y., Niu, H., Li, M., Yang, Y., Lu, S., Wu,

359 Y., Shao, M., and Shuai, S.: Potential of secondary aerosol formation from Chinese gasoline engine exhaust, Journal

360 of environmental sciences, 2017, in press.

361 Fu, H., Wang, Y., Li, X., and Shuai, S.: Impacts of Cold-Start and Gasoline RON on Particulate Emission from

362 Vehicles Powered by GDI and PFI Engines, SAE Technical Paper, 2014-01-2836, 10.4271/2014-01-2836, 2014.

363 Gao, Z., Curran, S. J., Parks, J. E., II, Smith, D. E., Wagner, R. M., Daw, C. S., Edwards, K. D., and Thomas, J. F.:

364 Drive cycle simulation of high efficiency combustions on fuel economy and exhaust properties in light-duty

365 vehicles, Applied Energy, 157, 762-776, 10.1016/j.apenergy.2015.03.070, 2015.

366 Gentner, D. R., Jathar, S. H., Gordon, T. D., Bahreini, R., Day, D. A., El Haddad, I., Hayes, P. L., Pieber, S. M.,

367 Platt, S. M., de Gouw, J., Goldstein, A. H., Harley, R. A., Jimenez, J. L., Prevot, A. S. H., and Robinson, A. L.:

368 Review of Urban Secondary Organic Aerosol Formation from Gasoline and Diesel Motor Vehicle Emissions,

369 Environmental science & technology, 51, 1074-1093, 10.1021/acs.est.6b04509, 2017.

Gordon, T. D., Presto, A. A., May, A. A., Nguyen, N. T., Lipsky, E. M., Donahue, N. M., Gutierrez, A., Zhang, M., Maddox, C., Rieger, P., Chattopadhyay, S., Maldonado, H., Maricq, M. M., and Robinson, A. L.: Secondary organic aerosol formation exceeds primary particulate matter emissions for light-duty gasoline vehicles, Atmos. Chem. Phys. , 14, 4661-4678, 10.5194/acp-14-4661-2014, 2014.

Guo, S., Hu, M., Zamora, M. L., Peng, J., Shang, D., Zheng, J., Du, Z., Wu, Z., Shao, M., Zeng, L., Molina, M. J., and Zhang, R.: Elucidating severe urban haze formation in China, Proceedings of the National Academy of Sciences of the United States of America, 111, 17373-17378, 10.1073/pnas.1419604111, 2014.

Hayes, P. L., Ortega, A. M., Cubison, M. J., Froyd, K. D., Zhao, Y., Cliff, S. S., Hu, W. W., Toohey, D. W., Flynn, J. H., Lefer, B. L., Grossberg, N., Alvarez, S., Rappenglueck, B., Taylor, J. W., Allan, J. D., Holloway, J. S., Gilman, J. B., Kuster, W. C., De Gouw, J. A., Massoli, P., Zhang, X., Liu, J., Weber, R. J., Corrigan, A. L., Russell, L. M., Isaacman, G., Worton, D. R., Kreisberg, N. M., Goldstein, A. H., Thalman, R., Waxman, E. M., Volkamer, R., Lin, Y. H., Surratt, J. D., Kleindienst, T. E., Offenberg, J. H., Dusanter, S., Griffith, S., Stevens, P. S., Brioude, J., Angevine, W. M., and Jimenez, J. L.: Organic aerosol composition and sources in Pasadena, California, during the 2010 CalNex campaign, Journal of Geophysical Research-Atmospheres, 118, 9233-9257, 10.1002/jgrd.50530, 2013.

Hays, M. D., Preston, W., George, B. J., Schmid, J., Baldauf, R., Snow, R., Robinson, J. R., Long, T., and Faircloth, J.: Carbonaceous aerosols emitted from light-duty vehicles operating on gasoline and ethanol fuel blends, Environmental science & technology, 47, 14502-14509, 10.1021/es403096v, 2013.

Hu, W., Hu, M., Hu, W., Jimenez, J. L., Yuan, B., Chen, W., Wang, M., Wu, Y., Chen, C., Wang, Z., Peng, J., Zeng, L., and Shao, M.: Chemical composition, sources, and aging process of submicron aerosols in Beijing: Contrast between summer and winter, Journal of Geophysical Research-Atmospheres, 121, 1955-1977, 10.1002/2015jd024020, 2016.

Huang, R.-J., Zhang, Y., Bozzetti, C., Ho, K.-F., Cao, J.-J., Han, Y., Daellenbach, K. R., Slowik, J. G., Platt, S. M., Canonaco, F., Zotter, P., Wolf, R., Pieber, S. M., Bruns, E. A., Crippa, M., Ciarelli, G., Piazzalunga, A., Schwikowski, M., Abbaszade, G., Schnelle-Kreis, J., Zimmermann, R., An, Z., Szidat, S., Baltensperger, U.,

Haddad, I. E., and Prévôt, A. S. H.: High secondary aerosol contribution to particulate pollution during haze events in China, Nature, 10.1038/nature13774, 2014.

Ito, Y., Shimoda, T., Aoki, T., Yuuki, K., Sakamoto, H., Kato, K., Their, D., Kattouah, P., Ohara, E. and Vogt, C.: Next Generation of Ceramic Wall Flow Gasoline Particulate Filter with Integrated Three Way Catalyst, SAE Technical Paper 2015-01-1073, 2015, doi:10.4271/2015-01-1073, 2015.

Jathar, S. H., Gordon, T. D., Hennigan, C. J., Pye, H. O. T., Pouliot, G., Adams, P. J., Donahue, N. M., and Robinson, A. L.: Unspeciated organic emissions from combustion sources and their influence on the secondary organic aerosol budget in the United States, Proc. Natl. Acad. Sci. USA, 111, 10473-10478, 10.1073/pnas.1323740111, 2014.

Jathar, S. H., Woody, M., Pye, H. O. T., Baker, K. R., and Robinson, A. L.: Chemical transport model simulations of organic aerosol in southern California: model evaluation and gasoline and diesel source contributions, Atmospheric Chemistry and Physics, 17, 4305-4318, 10.5194/acp-17-4305-2017, 2017.

Kamal, A., Cincinelli, A., Martellini, T., and Malik, R. N.: A review of PAH exposure from the combustion of biomass fuel and their less surveyed effect on the blood parameters, Environmental Science and Pollution Research, 22, 4076-4098, 10.1007/s11356-014-3748-0, 2015.

Kanakidou, M., Seinfeld, J. H., Pandis, S. N., Barnes, I., Dentener, F. J., Facchini, M. C., Van Dingenen, R., Ervens, B., Nenes, A., Nielsen, C. J., Swietlicki, E., Putaud, J. P., Balkanski, Y., Fuzzi, S., Horth, J., Moortgat, G. K., Winterhalter, R., Myhre, C. E. L., Tsigaridis, K., Vignati, E., Stephanou, E. G., and Wilson, J.: Organic aerosol and global climate modelling: a review, Atmospheric Chemistry and Physics, 5, 1053-1123, 2005.

Kramp, F., and Paulson, S. E.: On the uncertainties in the rate coefficients for OH reactions with hydrocarbons, and the rate coefficients of the 1,3,5-trimethylbenzene and m-xylene reactions with OH radicals in the gas phase, Journal of Physical Chemistry A, 102, 2685-2690, 10.1021/jp973289o, 1998.

Li, M., Hu, M., Wu, Y., Qin, Y., Zheng, R., Peng, J., Guo, Q., Xiao, Y., Hu, W., Zheng, J., Du, Z., Xiao, J., Shuai, S.: Characteristics of Particulate Organic Matters Emissions from Gasoline Direct Injection Engine and Its Influence Factors, Proceedings of the Chinese Society of Electrical Engineering, 36, 4443-4451.

419   Liang, B., Ge, Y., Tan, J., Han, X., Gao, L., Hao, L., Ye, W., and Dai, P.: Comparison of PM emissions from a

420   gasoline direct injected (GDI) vehicle and a port fuel injected (PFI) vehicle measured by electrical low pressure

421   impactor (ELPI) with two fuels: Gasoline and M15 methanol gasoline, Journal of Aerosol Science, 57, 22-31,

422   10.1016/j.jaerosci.2012.11.008, 2013.

423   Lindinger, W., Hansel, A., and Jordan, A.: On-line monitoring of volatile organic compounds at pptv levels by

424   means of proton-transfer-reaction mass spectrometry (PTR-MS) - Medical applications, food control and

425   environmental research, International Journal of Mass Spectrometry, 173, 191-241, 10.1016/s0168-

426   1176(97)00281-4, 1998.

427   Liu, T., Wang, X., Deng, W., Hu, Q., Ding, X., Zhang, Y., He, Q., Zhang, Z., Lü, S., Bi, X., Chen, J., and Yu, J.:

428   Secondary organic aerosol formation from photochemical aging of light-duty gasoline vehicle exhausts in a smog

429   chamber, Atmos. Chem. Phys. , 15, 9049-9062, 10.5194/acp-15-9049-2015, 2015.

430   Lu, K. D., Hofzumahaus, A., Holland, F., Bohn, B., Brauers, T., Fuchs, H., Hu, M., Häseler, R., Kita, K., Kondo,

431   Y., Li, X., Lou, S. R., Oebel, A., Shao, M., Zeng, L. M., Wahner, A., Zhu, T., Zhang, Y. H., and Rohrer, F.: Missing

432   OH source in a suburban environment near Beijing: observed and modelled OH and HO_2

433   concentrations in summer 2006, Atmos. Chem. Phys. , 13, 1057-1080, 10.5194/acp-13-1057-2013, 2013.

434   Maricq, M. M., Podsiadlik, D. H., and Chase, R. E.: Gasoline vehicle particle size distributions: Comparison of

435   steady state, FTP, and US06 measurements, Environmental science & technology, 33, 2007-2015,

436   10.1021/es981005n, 1999.

437   Mathis, U., Mohr, M., and Forss, A. M.: Comprehensive particle characterization of modern gasoline and diesel

438   passenger cars at low ambient temperatures, Atmospheric Environment, 39, 107-117,

439   10.1016/j.atmosenv.2004.09.029, 2005.

440   May, A. A., Nguyen, N. T., Presto, A. A., Gordon, T. D., Lipsky, E. M., Karve, M., Gutierrez, A., Robertson, W. H.,

441   Zhang, M., Brandow, C., Chang, O., Chen, S., Cicero-Fernandez, P., Dinkins, L., Fuentes, M., Huang, S.-M., Ling,

442   R., Long, J., Maddox, C., Massetti, J., McCauley, E., Miguel, A., Na, K., Ong, R., Pang, Y., Rieger, P., Sax, T., Tin,

443   T., Thu, V., Chattopadhyay, S., Maldonado, H., Maricq, M. M., and Robinson, A. L.: Gas- and particle-phase

444   primary emissions from in-use, on-road gasoline and diesel vehicles, Atmospheric Environment, 88, 247-260,

445   10.1016/j.atmosenv.2014.01.046, 2014.

446   Myung, C.-L., Kim, J., Choi, K., Hwang, I. G., and Park, S.: Comparative study of engine control strategies for

447   particulate emissions from direct injection light-duty vehicle fueled with gasoline and liquid phase liquefied

448   petroleum gas (LPG), Fuel, 94, 348-355, 10.1016/j.fuel.2011.10.041, 2012.

449   Ng, N. L., Kroll, J. H., Chan, A. W. H., Chhabra, P. S., Flagan, R. C., and Seinfeld, J. H.: Secondary organic aerosol

450   formation from m-xylene, toluene, and benzene, Atmos. Chem. Phys. , 7, 3909–3922, 2007.

451   Nordin, E. Z., Eriksson, A. C., Roldin, P., Nilsson, P. T., Carlsson, J. E., Kajos, M. K., Hellén, H., Wittbom, C.,

452   Rissler, J., Löndahl, J., Swietlicki, E., Svenningsson, B., Bohgard, M., Kulmala, M., Hallquist, M., and Pagels, J.

453   H.: Secondary organic aerosol formation from idling gasoline passenger vehicle emissions investigated in a smog

454   chamber, Atmos. Chem. Phys. , 13, 6101-6116, 10.5194/acp-13-6101-2013, 2013.

455   Odum, J. R., Hoffmann, T., Bowman, F., Collins, D., Flagan, R. C., and Seinfeld, J. H.: Gas/particle partitioning

456   and secondary organic aerosol yields, Environ. Sci. Technol., 30, 2580-2585, 10.1021/es950943+, 1996.

457   Peng, J., Hu, M., Du, Z., Wang, Y., Zheng, J., Zhang, W., Yang, Y., Qin, Y., Zheng, R., Xiao, Y., Wu, Y., Lu, S., Wu,

458   Z., Guo, S., Mao, H., and Shuai, S.: Gasoline aromatic: a critical determinant of urban secondary organic aerosol

459   formation, Atmospheric Chemistry and Physics, 2017, in press.

460   Platt, S. M., El Haddad, I., Zardini, A. A., Clairotte, M., Astorga, C., Wolf, R., Slowik, J. G., Temime-Roussel, B.,

461   Marchand, N., Ježek, I., Drinovec, L., Močnik, G., Möhler, O., Richter, R., Barmet, P., Bianchi, F., Baltensperger,

462   U., and Prévôt, A. S. H.: Secondary organic aerosol formation from gasoline vehicle emissions in a new mobile

463   environmental reaction chamber, Atmos. Chem. Phys. , 13, 9141-9158, 10.5194/acp-13-9141-2013, 2013.

464   Robinson, A. L., Donahue, N. M., Shrivastava, M. K., Weitkamp, E. A., Sage, A. M., Grieshop, A. P., Lane, T. E.,

465   Pierce, J. R., and Pandis, S. N.: Rethinking organic aerosols: Semivolatile emissions and photochemical aging,

466   Science, 315, 1259-1262, 10.1126/science.1133061, 2007.

467   Saliba, G., Saleh, R., Zhao, Y., Presto, A. A., Lambe, A. T., Frodin, B., Sardar, S., Maldonado, H., Maddox, C.,

468   May, A. A., Drozd, G. T., Goldstein, A. H., Russell, L. M., Hagen, F., and Robinson, A. L.: Comparison of Gasoline

469   Direct-Injection (GDI) and Port Fuel Injection (PFI) Vehicle Emissions: Emission Certification Standards, Cold-

470   Start, Secondary Organic Aerosol Formation Potential, and Potential Climate Impacts, Environmental science &

471   technology, 51, 6542-6552, 10.1021/acs.est.6b06509, 2017.

472   Schauer, J. J., Kleeman, M. J., Cass, G. R. and Simoneit, B. R. T.: Measurement of Emissions from Air Pollution

473   Sources. 5. C1-C32 Organic Compounds from Gasoline-Powered Motor Vehicles, Environmental science &

474   technology, 36, 1169-1180, 2002.

475   Seinfeld, J. H., Kleindienst, T. E., Edney, E. O., and Cohen, J. B.: Aerosol growth in a steady-state, continuous flow

476   chamber: Application to studies of secondary aerosol formation, Aerosol Science and Technology, 37, 728-734,

477   10.1080/02786820390214954, 2003.

478   Song, C., Na, K. S., and Cocker, D. R.: Impact of the hydrocarbon to NOx ratio on secondary organic aerosol

479   formation, Environ. Sci. Technol., 39, 3143-3149, 10.1021/es0493244, 2005.

480   Ueberall, A., Otte, R., Eilts, P., and Krahl, J.: A literature research about particle emissions from engines with direct

481   gasoline injection and the potential to reduce these emissions, Fuel, 147, 203-207, 10.1016/j.fuel.2015.01.012,

482   2015.

483   Wang, Y., Zheng, R., Qin, Y., Peng, J., Li, M., Lei, J., Wu, Y., Hu, M., and Shuai, S.: The impact of fuel compositions

484   on the particulate emissions of direct injection gasoline engine, Fuel, 166, 543-552, 10.1016/j.fuel.2015.11.019,

485   2016.

486   Wang, Z. B., Hu, M., Wu, Z. J., Yue, D. L., He, L. Y., Huang, X. F., Liu, X. G., and Wiedensohler, A.: Long-term

487   measurements of particle number size distributions and the relationships with air mass history and source

488   apportionment in the summer of Beijing, Atmospheric Chemistry and Physics, 13, 10159-10170, 10.5194/acp-13-

489   10159-2013, 2013.

490   Wen, Y., Wang, Y., Fu, C., Deng, W., Zhan, Z., Tang, Y., Li, X., Ding, H., and Shuai, S.: The Impact of Injector

491   Deposits on Spray and Particulate Emission of Advanced Gasoline Direct Injection Vehicle, SAE Technical Paper,

492   2016-01-2284, 10.4271/2016-01-2284, 2016.

493   Yang, B., Ma, P. K., Shu, J. N., Zhang, P., Huang, J. Y. and Zhang, H. X.: Formation mechanism of secondary

494   organic aerosol from ozonolysis of gasoline vehicle exhaust, Environmental Pollution, 234, 960-968,

495   10.1016/j.envpol.2017.12.048, 2018.

496   Yuan, B., Shao, M., de Gouw, J., Parrish, D. D., Lu, S., Wang, M., Zeng, L., Zhang, Q., Song, Y., Zhang, J., and

497   Hu, M.: Volatile organic compounds (VOCs) in urban air: How chemistry affects the interpretation of positive

498   matrix factorization (PMF) analysis, Journal of Geophysical Research: Atmospheres, 117, n/a-n/a,

499   10.1029/2012jd018236, 2012.

500   Zhang, Q., Jimenez, J. L., Canagaratna, M. R., Allan, J. D., Coe, H., Ulbrich, I., Alfarra, M. R., Takami, A.,

501   Middlebrook, A. M., Sun, Y. L., Dzepina, K., Dunlea, E., Docherty, K., DeCarlo, P. F., Salcedo, D., Onasch, T.,

502   Jayne, J. T., Miyoshi, T., Shimono, A., Hatakeyama, S., Takegawa, N., Kondo, Y., Schneider, J., Drewnick, F.,

503   Borrmann, S., Weimer, S., Demerjian, K., Williams, P., Bower, K., Bahreini, R., Cottrell, L., Griffin, R. J.,

504   Rautiainen, J., Sun, J. Y., Zhang, Y. M., and Worsnop, D. R.: Ubiquity and dominance of oxygenated species in

505   organic aerosols in anthropogenically-influenced Northern Hemisphere midlatitudes, Geophysical Research Letters,

506   34, 10.1029/2007gl029979, 2007.

507   Zhang, X., Cappa, C. D., Jathar, S. H., McVay, R. C., Ensberg, J. J., Kleeman, M. J., and Seinfeld, J. H.: Influence

508   of vapor wall loss in laboratory chambers on yields of secondary organic aerosol, Proc. Natl. Acad. Sci. USA, 111,

509   5802-5807, 10.1073/pnas.1404727111, 2014.

510   Zhao, Y., Nguyen, N. T., Presto, A. A., Hennigan, C. J., May, A. A., and Robinson, A. L.: Intermediate Volatility

511   Organic Compound Emissions from On-Road Gasoline Vehicles and Small Off-Road Gasoline Engines,

512   Environmental science & technology, 50, 4554-4563, 10.1021/acs.est.5b06247, 2016.

513   Zhao, Y., Saleh, R., Saliba, G., Presto, A. A., Gordon, T. D., Drozd, G. T., Goldstein, A. H., Donahue, N. M., and

514   Robinson, A. L.: Reducing secondary organic aerosol formation from gasoline vehicle exhaust, Proceedings of the

515   National Academy of Sciences of the United States of America, 114, 6984-6989, 10.1073/pnas.1620911114, 2017.

516   Zhu, R., Hu, J., Bao, X., He, L., Lai, Y., Zu, L., Li, Y., and Su, S.: Tailpipe emissions from gasoline direct injection

517   (GDI) and port fuel injection (PFI) vehicles at both low and high ambient temperatures, Environmental Pollution,

518   216, 223-234, 10.1016/j.envpol.2016.05.066, 2016.

519   Zimmerman, N., Wang, J. M., Jeong, C.-H., Ramos, M., Hilker, N., Healy, R. M., Sabaliauskas, K., Wallace, J. S.,

520   and Evans, G. J.: Field Measurements of Gasoline Direct Injection Emission Factors: Spatial and Seasonal

521   Variability, Environmental science & technology, 50, 2035-2043, 10.1021/acs.est.5b04444, 2016.

522

523 Table 1 Descriptions of the gasoline direct injection (GDI) and port fuel injection (PFI) vehicles used in the

524 experiments.

Vehicle	Make and model	Emission standard class	Model year	Mileage (km)	Displacement (cm³)	Power (kW)	Weight (kg)
GDI	VW Sagitar	China V	2015	3000	1395	110	1395
PFI	Honda Civic	China IV	2009	42500	1799	103	1280

525

526 Table 2 Overview of all instruments used to measure the gas and particulate phase pollutants in the experiments.

Parameter	Phase	Instrument	Note
CO, CO$_2$, NO$_x$ and total hydrocarbon (THC) concentration	Gas	Gas analyzer AVL Combustion Emissions Bench II	On-line
Aerosol number size distribution	Particle	DMS500	On-line
PM$_{2.5}$	Particle	Balance (AX105DR)	Off-line
Organic carbon/Elemental carbon concentration	Particle	OC/EC analyzer	Off-line
CO concentration	Gas	48i CO analyzer	On-line
NO, NO$_2$, and NO$_x$ concentration	Gas	42i NO-NO$_2$-NO$_x$ analyzer	On-line
O$_3$ concentration	Gas	49i O$_3$ analyzer	On-line
VOCs concentration	Gas	Proton transfer reaction mass spectrometer (PTR-MS)	On-line
Aerosol number (mass) size distribution	Particle	Scanning mobility particle sizer (SMPS, consist of 3081-DMA and 3775-CPC),	On-line
Size resolved non-refractory aerosol	Particle	High resolution time-of-flight aerosol mass spectrometer (HR-Tof-AMS)	On-line

527

528

24

529 Table 3 Emission factors (EFs) of gaseous pollutants from the gasoline direct injection (GDI) and port fuel injection (PFI) vehicles in

530 this study and those of previous studies.

	This study				Saliba et al., 2017		May et al., 2014	Platt et al., 2013		Zhu et al., 2016	
	GDI		PFI		GDI	PFI	PFI[a]			GDI	PFI
	China V		China IV		ULEV	ULEV	LEV II	Euro V		China IV	China IV
	Cold BJC				Cold UC[b]		Cold UC	Cold NEDC		Cold WLTC[c]	
	g kg-fuel^{-1}	g km^{-1}	g kg-fuel^{-1}	g km^{-1}	g km^{-1}	g km^{-1}	g kg-fuel^{-1}	g kg-fuel^{-1}	g km^{-1}	g km^{-1}	g km^{-1}
CO_2	3439 ±23	213 ±4	3350 ±24	283 ±4	-	-	-	-	-	187	215
THC	1.55 ±0.22	0.09 ±0.01	1.70 ±0.19	0.13 ±0.01	0.02	0.06	0.64	0.91-1.06	0.036-0.042	0.05	0.03
Benzene	0.056 ±0.011	0.003 ±0.001	0.061 ±0.016	0.005 ±0.001	-	-	0.018	-	0.002	-	-
Toluene	0.101 ±0.004	0.006 ±0.001	0.220 ±0.047	0.017 ±0.004	-	-	0.026	-	0.002	-	-

531 [a] 22 PFI vehicles and 3 GDI vehicles;

532 [b] UC: Unified Cycle;

533 [c] WLTC: Worldwide-harmonized Light-duty Test Cycle

534   Table 4 EFs of primary aerosols, including carbonaceous aerosols and particulate polycyclic aromatic hydrocarbons (PAHs) from the

535   GDI and PFI vehicles in this study and those of previous studies.

	This study				Saliba et al., 2017		May et al., 2014	Platt et al., 2013		Zhu et al., 2016	
	GDI		PFI		GDI	PFI	PFI			GDI	PFI
	China V		China IV		ULEV	ULEV	LEV II	Euro V		China IV	China IV
	Cold BJC				Cold UC		Cold UC	Cold NEDC		Cold WLTC	
	mg kg-fuel^{-1}	mg km^{-1}	mg kg-fuel^{-1}	mg km^{-1}	mg km^{-1}	mg km^{-1}	mg kg-fuel^{-1}	mg kg-fuel^{-1}	mg km^{-1}	mg km^{-1}	mg km^{-1}
PM$_{2.5}$	61.7±24.5	3.4±1.4	33.4±25.6	2.5±1.9	3.9	2.4	18.0	-	-	1.5	1.0
EC	10.7±3.6	0.6±0.2	2.4±1.6	0.2±0.1	3.0	0.6	12.2	11.2-20.0	1.2-1.7	-	-
POA	41.7±9.8	2.3±0.6	25.0±0.3	1.9±0.1	0.4	0.6	5.2	24.5-19.7	0.4-1.4	-	-
OC/EC	3.2		8.7		0.1	0.8	0.4	0.2-1.8		-	-
PAHs(×10^6)	20.4±2.1	1.1±0.1	13.2±4.1	1.0±0.3	-	-	-	-	-	-	-

536

537

538

Figure 1. Schematic diagram of the outdoor chamber set up for the experiments.

540

541

542　Figure 2. Number size distributions of primary PM emitted from the GDI (red line) and PFI (blue line) gasoline

543　vehicles. The results are average of particle number emissions from vehicles during a whole BJC, measured by

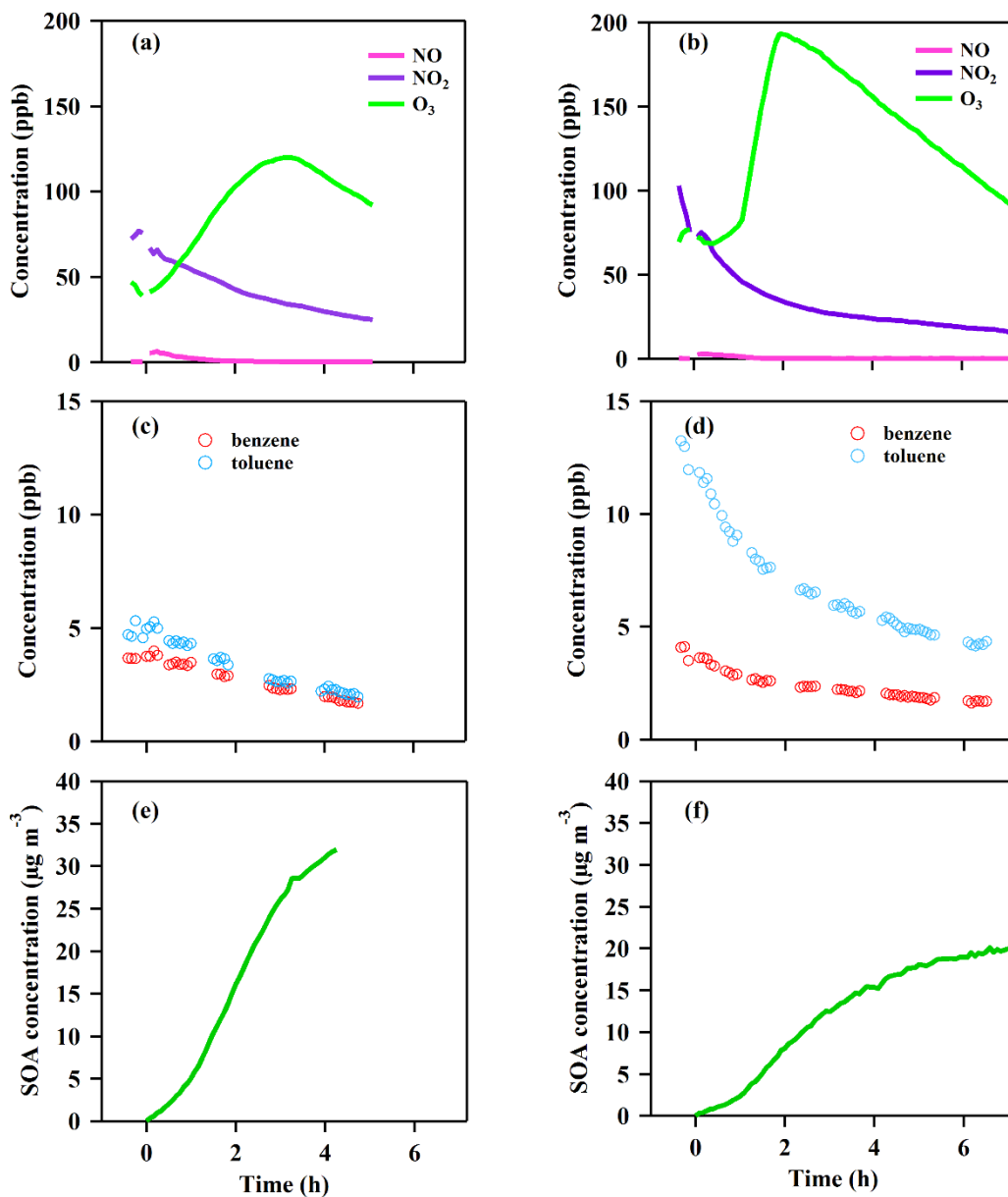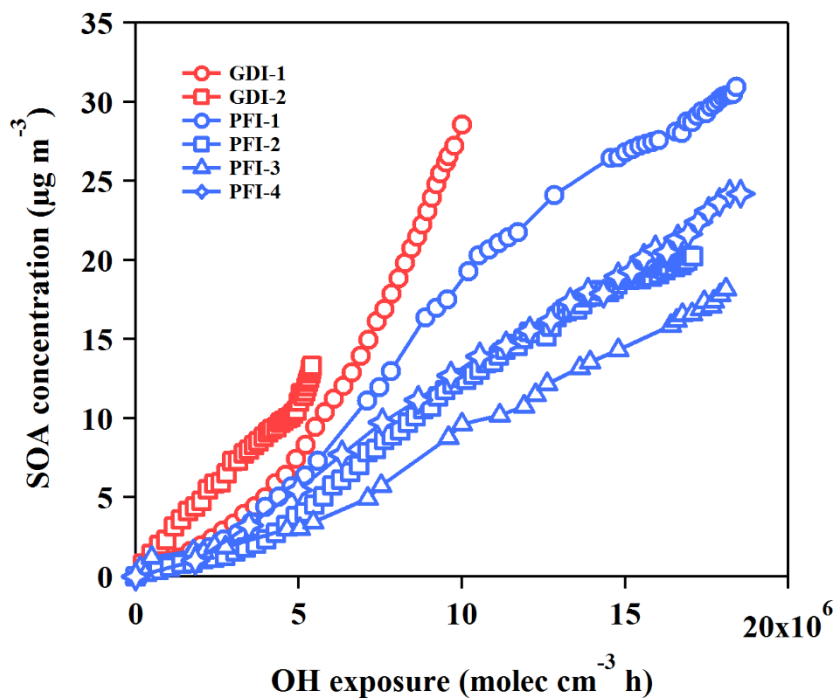544　DMS500 in the CVS system. The particles were heated to 150℃ in the DMS500.

545

546

Figure 3. Time series of the gases and particle evolutions over the photochemical age in the chamber experiments

from the GDI vehicle exhaust (a, c, e) and PFI vehicle exhaust (b, d, f). (a, b): NO, NO_2 and O_3 concentration; (c,

d): benzene and toluene concentration; (e, f): corrected SOA concentration.

551

Figure 4. SOA productions from the GDI vehicle exhaust (red markers) and the PFI vehicle exhaust (blue markers)
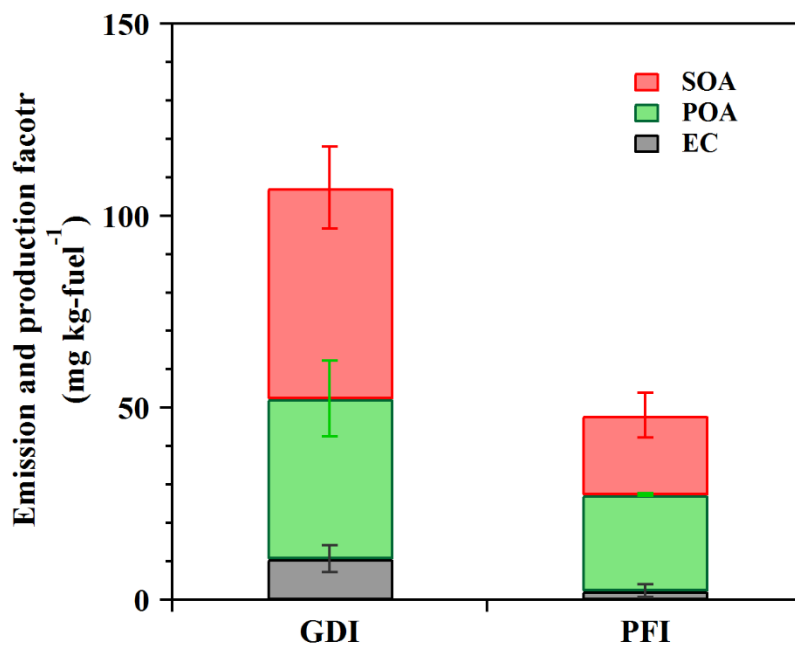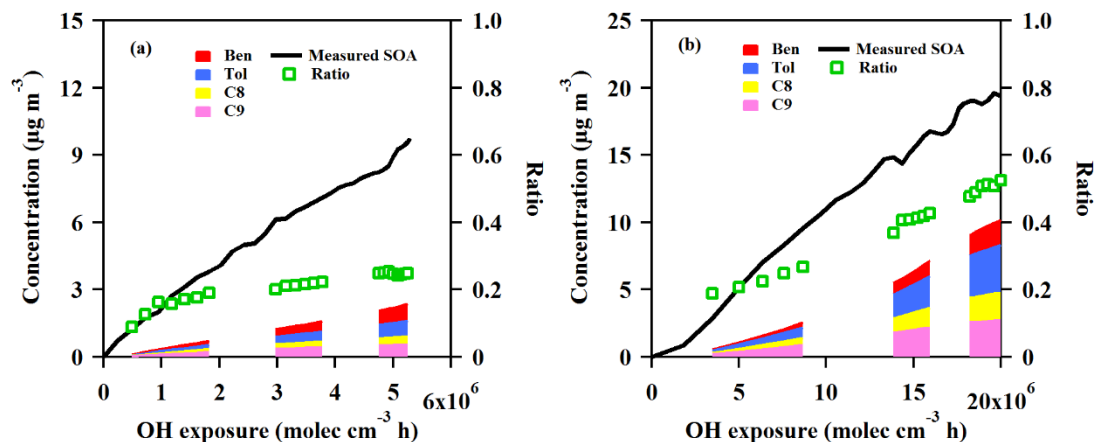
as functions of OH exposure in the chamber experiments.

554

555

Figure 5. Fuel-based SOA production from gasoline vehicle exhaust as a function of OH exposure in the chamber

simulations. The SOA production data are from published studies of chamber simulation of gasoline vehicle

exhaust. From the study of Jathar et al. (2014), the SOA production of vehicles manufactured in 2004 or later (LEV

II) is selected, which is a model year that is more close to those of the vehicles in this study. The error bars of

previous results indicate the range of OH exposure (x axis) and SOA production (y axis) in their simulations. The

driving cycles and vehicle information are also noted in the legend of each study.

562

31

563

Figure 6 EC and POA EFs as well as corrected SOA production factors from the GDI and PFI vehicle exhausts in
this study (OH exposure = 5×10^6 molecular cm^{-3} h).

566

567

Figure 7. Measured and predicted SOA concentration as a function of OH exposure from GDI vehicle exhaust (a) and PFI vehicle exhaust (b) in the chamber experiments. The black line is the measured SOA concentration with wall-loss and particle dilution correction during the experiment. The red, blue, yellow and pink areas are predicted SOA concentration estimated from benzene, toluene, C8 benzene and C9 benzene, respectively. The green markers are the ratios of the predicted SOA to the measured SOA.

1 **Supplementary information**

2 **Comparison of primary aerosol emission and secondary aerosol formation from gasoline**

3 **direct injection and port fuel injection vehicles**

4 Zhuofei Du[1], Min Hu[1, 3*], Jianfei Peng[1†], Wenbin Zhang[2], Jing Zheng[1], Fangting Gu[1], Yanhong

5 Qin[1], Yudong Yang[1], Mengren Li[1], Yusheng Wu[1], Min Shao[1], Shijin Shuai[2]

6 1. State Key Joint Laboratory of Environmental Simulation and Pollution Control, College of

7 Environmental Sciences and Engineering, Peking University, Beijing 100871, China

8 2. State Key Laboratory of Automotive Safety and Energy, Department of Automotive

9 Engineering, Tsinghua University, Beijing 100084, China

10 3. Beijing Innovation Center for Engineering Sciences and Advanced Technology, Peking

11 University, Beijing 100871, China

12 [†] Now at Department of Atmospheric Sciences, Texas A&M University, College Station, TX

13 77843, US

14

15 *Corresponding author: Min Hu, minhu@pku.edu.cn

16

Data correction

Wall-loss correction as well as particle and gas dilution corrections were considered in this study. The details of wall-loss correction are introduced by Du et al. (2017). The real-time instruments sampled from the chamber during the whole photo-oxidation experiment, and zero air was added to maintain a constant pressure inside the chamber. This led to particle dilution that the sampled particles would not be included in the subsequent measurement, and gas dilution that the sampled gas would not participate in the subsequent photo-oxidation reaction and SOA formation. The particle dilution corrected mass concentration $C_{corr,n+1}$ could be calculated as:

$$C_{corr,n+1} = C_{n+1} + \sum_{i=1}^{n}(k_{wall} \times C_i) + \sum_{i=1}^{n}(k_{dilu,i} \times C_i) \tag{1}$$

where C_{n+1} was the measured particle mass concentration at time n+1, k_{wall} was the wall loss decay constant and $k_{dilu,i}$ was dilution ratio at time i.
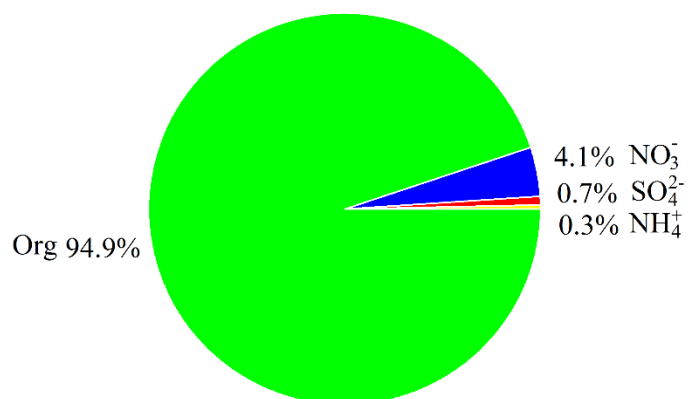
Then the gas dilution was taken into consideration. The final particle mass concentration $C_{final,n+1}$ could be calculated as:

$$C_{final,n+1} = C_{corr,n+1} - C_1 + \sum_{i=1}^{n}\left(\sum_{i=1}^{n+1} k_{dilu,i}\right) \times (C_{corr,n+1} - C_{corr,n}) \tag{2}$$

References

Du, Z., Hu, M., Peng, J., Guo, S., Zheng, R., Zheng, J., Shang, D., Qin, Y., Niu, H., Li, M., Yang, Y., Lu, S., Wu, Y., Shao, M., and Shuai, S.: Potential of secondary aerosol formation from Chinese gasoline engine exhaust, Journal of environmental sciences, in press.
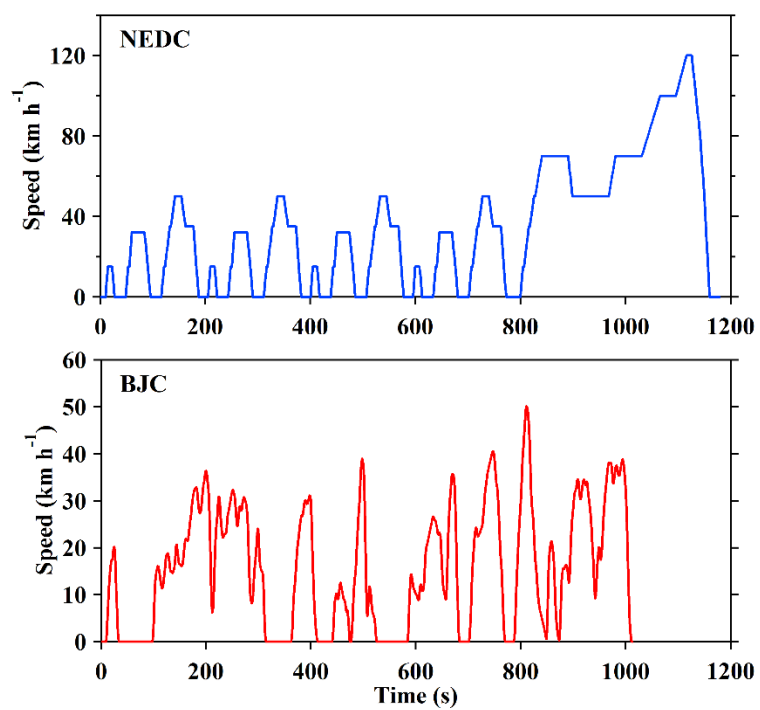
40

The pie chart shows:
- Org 94.9% (green)
- 4.1% NO_3^-
- 0.7% SO_4^{2-}
- 0.3% NH_4^+

41

Figure S1. Chemical composition of secondary aerosol formed in the chamber experiment

(Experiment GDI-1).

44

45

46

Figure S2. Speed profiles of NEDC and BJC driving cycle.

48

49   Table S1 Details of the fuel used in the experiments.

Specifications	Fuel
Density (g mL^{-1})	0.7
Rvp (kPa)	55.4
Aromatics (% v/v)	36.7
Olefin (% v/v)	15.4
Ethanol (% v/v)	0.01
Oxygen (% m/m)	0.02
Mn (mg kg^{-1})	< 0.1
Sulfur (mg kg^{-1})	6
T10 (℃)	55.4
T50 (℃)	109.9
T90 (℃)	164.3
Fbp (℃)	194.4

50

51

52   Table S2 The EFs of Particulate-phase PAHs from GDI and PFI vehicles.

Compound	Emission factor (ng kg-fuel^{-1})	
	GDI	PFI
Napthalene	0.025	<0.0001
1-Methylnaphthalene	<0.0001	<0.0001
2-Methylnaphthalene	0.012	0.004
2,6-Dimethylnaphthalene	0.006	0.003
Acenaphthylene	0.012	0.009
Acenapthene	<0.0001	0.015
Fluorene	0.003	0.105
Methyl-fluorene	0.083	0.105
Dibenzofuran	0.006	0.039
Retene	0.009	0.011
9-Methylanthracene	<0.0001	0.013
Phenanthrene	0.244	0.069
Anthracene	0.048	0.018
Fluoranthene	0.201	0.034
Pyrene	0.246	0.029
Methyl-fluoranthene	0.004	0.007
Benzo[a]anthracene	0.006	0.036
Chrysene	0.020	0.065
Methyl-chrysene	<0.0001	0.007
Benzo[b]fluoranthene	0.034	0.147
Benzo[k]fluoranthene	0.041	0.129
Benzo[e]pyrene	0.028	0.051
Benzo[a]pyrene	0.012	0.041
Benzo[ghi]flouranthene	0.095	0.027
Cyclopenta[cd]pyrene	<0.0001	0.032
Dibenzo[a,h]anthracene	<0.0001	<0.0001

Picene	<0.0001	<0.0001
Perylene	0.009	<0.0001
Benzo[ghi]perylene	<0.0001	<0.0001
Indeno[1,2,3-cd]pyrene	<0.0001	<0.0001
Coronene	<0.0001	<0.0001
Sum PAHs	1.144	0.994

53

Response to Comments by Referee #2

Thank you for your commendation and appreciate your suggestions on all scientific, technical aspects of our article. The manuscript has been revised accordingly. Listed below is our point-to-point response to each comment.

Du et al. report on emissions and chamber experiments performed on port fuel injection (PFI) and gasoline direct injection (GDI) gasoline vehicles and their potential to form secondary organic aerosol (SOA). They find that the PFI vehicle emits more VOCs compared to the GDI vehicle but the GDI vehicle emits both primary particles and forms more SOA than the PFI vehicle. They claim that the higher SOA from GDI vehicles could be attributed to higher emissions of intermediate volatility organic compounds (IVOCs).

The study builds on previous work done with PFI and GDI vehicles to answer an important question currently on the minds of researchers and regulators: are GDI vehicles a cause for more primary and secondary pollution in the future? Thus, the work is well-motivated and very topical. The manuscript could benefit from a copyedit from someone with fluency in English since there are some styling and phrasing issues. The methods are appropriate and the experimental results are worth publishing although there are some minor issues that need to be resolved (see comments below). My major concern is the study design that only used one vehicle of each technology type and that the conclusions are generalized for all vehicles in that technology type. I recommend publication after the authors have had an opportunity to respond to my comments.

Major comment:

Vehicle-to-vehicle variability - Vehicles certified to the same emissions standard can vary significantly in their tailpipe emissions and their potential to form SOA (order of magnitude or more). For example, see any of the large studies done over the past decade and a half (Kishan et al., 2008; May et al., 2014). In the United States where successive emissions standards for any given pollutant do not change by an order of magnitude, it follows then that it is likely that a randomly picked vehicle certified to a newer standard emits more pollutants than a randomly picked vehicle certified to an older standard. In the context of this work then, one needs to be careful in comparing absolute emissions/production from one PFI vehicle against another GDI vehicle and using those comparisons to make broader conclusions about PFI versus GDI vehicles. For example, it is imprecise to imply that all GDI vehicles had higher SOA production factors than PFI vehicles (as mentioned in the title) or that the GDI versus PFI SOA difference could be attributed to higher S/IVOC emissions (as mentioned in the discussion section). If this study would have included many more vehicles or somehow performed on the same vehicle but with interchangeable injection methods, this comment would not apply but since only one vehicle was chosen for each technology type this becomes a concern. Can the authors comment on why the vehicles they picked are representative of their technology type and why the differences from those vehicles (e.g., Table 3 and 4) can be extrapolated to a whole class of vehicles?

Response: We thank the reviewer for reminding this. The GDI and PFI vehicles chosen in this study have high market share of on-road gasoline vehicles in China. We agree with the referee that one vehicle for each gasoline engine technology exists uncertainty, and more researches with more vehicles will be conducted in the future. The title and discussions are revised as the suggestion.

The title is revised as: "Comparison of primary aerosol emission and secondary aerosol formation from gasoline direct injection and port fuel injection vehicles".

Following discussion is added between Line 312 to Line 315: "It should be pointed out that the SOA formation factors in this study are only based on only one GDI vehicle and one PFI vehicle. For vehicles with similar specification using the same fuel, some previous studies show that their emissions have some variations (Gordon et al., 2014; Jathar et al., 2014). Thus more researches of more vehicles for each technology are needed on SOA formation from vehicle exhaust".

Specific comments:

1. Line 34-44: There is a lot more modeling and measurement work done around understanding the motor vehicle contribution to OA in urban areas. Perhaps work on a better literature review to motivate the work?

Response: Thanks for the suggestion. More previous studies on vehicles contribution to urban OA are added, and the literature review is revised as:

Line 34 to Line 48: "Organic aerosols account for approximately 20-50 % of ambient fine particulate matter (PM2.5), with significant environment and health effects (Kanakidou et al., 2005). Primary organic aerosol (POA) is emitted directly by sources, while secondary organic aerosol (SOA) is mainly formed via oxidation of gaseous precursors in the atmosphere and account for about 30-90 % of the organic aerosol (OA) mass worldwide (Zhang et al., 2007; Hu et al., 2016), but SOA source remain poorly constrained. Robinson et al. (2007) proposed that low-volatility gas-phase species emitted from diesel vehicles were important sources for urban ambient SOA, which achieved better mass closure between observed and modeled SOA. Using an updated CMAQ model, Jathar et al. (2017) found that 30-40% OA was contributed from vehicles in the southern California, and half of which was SOA. Huang et al. (2014) recently revealed that 15-65 % of SOA was contributed by fossil fuel consumption (i.e., traffic and coal burning) in megacities in China. These indicated that vehicles have important contribution to ambient SOA in urban areas. An ambient organic aerosol measurement in the Los Angeles Basin demonstrated that SOA contributed from gasoline vehicles was significant in the urban air, much larger than that from diesel vehicles (Bahreini et al., 2012). Similar conclusion was reached by Hayes et al. (2013) based on mass spectrometer results. Meanwhile, several chamber simulation studies concluded that exhaust of gasoline vehicles could form substantial SOA (Jathar et al., 2014). Thus, gasoline vehicles exhaust is highly associated with ambient SOA formation".

2. Line 40: Does Huang et al. (2014) only refer to Chinese cities?

Response: Huang et al. (2014) refers to Beijing, Xi'an, Shanghai and Guangzhou four Chinese cities. More literatures on other cities were added between Line 38 to Line 41: "Robinson et al. (2007)

proposed that low-volatility gas-phase species emitted from diesel vehicles were important sources for urban ambient SOA, which achieved better mass closure between observed and modeled SOA. Using an updated CMAQ model, Jathar et al. (2017) found that 30-40% OA was contributed from vehicles in the southern California, and half of which was SOA".

3. Line 42: 'exhaust' not 'exhausts'.

Response: Thanks for the advice. Modified as suggested.

4. Line 47-49: In comparison to what type of vehicle? My understanding is that one of the major advantages of the GDI is that it eliminates pumping losses.

Response: Thanks for the advice. The GDI vehicle is compared to PFI vehicle based on their engine technologies. The less fuel pumping loss of GDI engine is added between Line 52 to Line 54: "... a GDI engine has many advantages, such as better fuel efficiency, lower CO2 emissions and less fuel pumping loss (Alkidas, 2007; Myung et al., 2012; Liang et al., 2013)".

5. Line 51-52: Are these percentages for sales of new vehicles only?

Response: These percentages refer to market shares of sales. The sentence is revised as follows: Line 56 to Line 57: "The market share of GDI vehicles in sales in 2016 reached about 25 %, 50 % and 60 % in China, the US and Europe, respectively (Wen et al., 2016; Zimmerman et al., 2016)".

6. Line 67: Gentner et al. (2017) is a review paper. Please state the primary study.

Response: We thank the referee for pointing out this. The reference is revised, and the sentence is modified as follows:
Line 69 to Line 72: These studies mostly focused on the impacts of SOA formation by the model year (Gordon et al., 2014; Jathar et al., 2014; Liu et al., 2015), fuel formulations (Peng et al., 2017), driving cycles (including idling) (Nordin et al., 2013; Platt et al., 2013) and start-up modes of the gasoline vehicles (Nordin et al., 2013).

7. Line 72: 'formation' not 'formations'.

Response: Thanks for the advice. Modified as suggested.

8. Line 89: How many experiments were performed? Figure 4 suggests two for the GDI and four for the PFI. Mention this in the methods section.

Response: Thanks for the suggestion. Six chamber experiments, including two for the GDI vehicle and four for the PFI vehicle, were conducted in this study. A sentence is added between Line 96 to Line 98 to make it clear:

"The chamber experiments were carried out in the summer at the State Key Laboratory of Automotive Safety and Energy of Tsinghua University in Beijing, including two experiments conducted with GDI vehicle and four experiments conducted with PFI vehicle".

9. Line 97-99: How was the setup designed to reduce losses of gases and particles from the CVS to the chamber? Were the transfer lines heated? Were they coated to reduce losses of vapors and particles? How long were the transfer lines? Were the gas and particle losses in the transfer line characterized before performing the vehicle experiments?

Response: Thanks. Due to the short transfer tube from the CVS to the chamber (1-1.5 m) and high flowrate, residence time was short, and loss of vapor as well as particles was low. So the exhaust was controlled as room temperature 26.4±2.5 ℃ without heating.

10. Line 110-111: How were the concentration data corrected for additional dilution?

Response: The flowrate of zero air added to chamber is equal to that of instruments sampling from chamber during that time. So the known volume of zero air is involved in the dilution calculation.

11. Does a DMS500 thermally denude the particles before measurement? This should be mentioned. Also, what is the denuding temperature?

Response: We thank the referee for pointing out these. The sampling line of DMS500 is heated to 150℃. The information is added between Line 125 to Line 126: "Its sampling line was heated to maintain the temperature at 150℃".

12. Line 147-148: Are the BJC versus NEDC differences shown in this work?

Response: Thanks for the advice. The speed profiles of BJC and NEDC driving cycle are added in the Supplement as Figure S2.
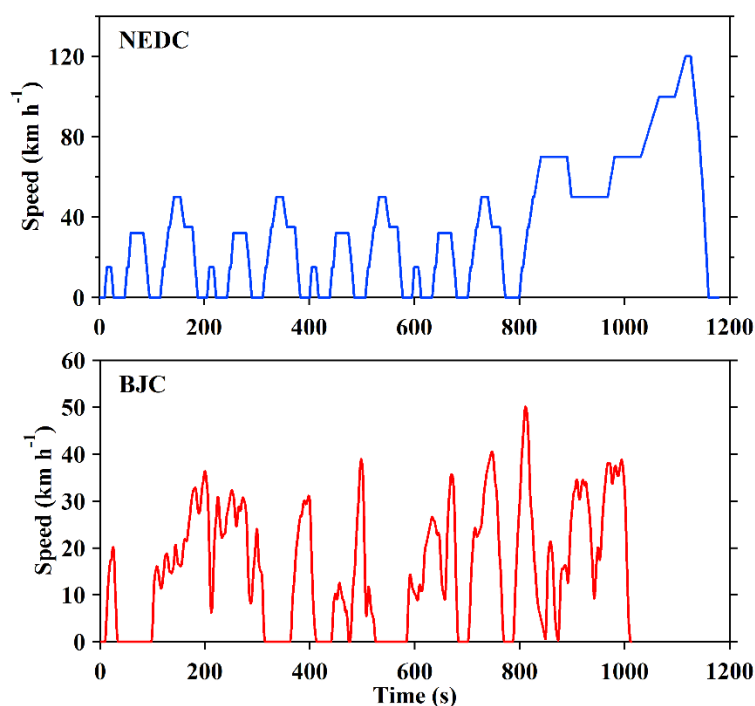
Figure S2. Speed profiles of NEDC and BJC driving cycle.

13. Line 150: What was the benzene to toluene ratio in the fuel and does this align with the emissions measurements?

Response: The toluene to benzene ratio is about 1000 in the fuel. The ratio in the fuel showing significantly higher than that in the exhaust, might due to many complex procedures during fuel combustion.

14. Line 166: What was the EC+POA mass compared to? Teflon filters? Were artifacts on the Quartz filters considered in the comparison? What OM to OC ratio was used to get POA mass?

Response: The EC+POA mass was compared to PM2.5 measured by Teflon filters. The AVL Particulate Sampling System was equipped with a denuder (filled with activated carbon) to remove organic vapors, preventing organic vapors condensing on the Quartz filters.
The OM/OC ratio of 1.2 was applied to get POA mass, representing emissions of fresh vehicle (Saliba et al., 2017).

15. Line 172: POA was not higher in Saliba et al. (2017) only EC was.

Response: We apologize for the mistake. The sentence is revised as:
Line 184 to Line 186: "The lower PM2.5 and POA emissions from GDI vehicle were found in previous studies, except that a little higher PM2.5 emission from GDI vehicle was illustrated in

Saliba's study (Platt et al., 2013; May et al., 2014; Zhu et al., 2016; Saliba et al., 2017)".

16. Line 181-184: The tailpipe aerosol size distribution can vary substantially with atmospheric processes (e.g., coagulation, evaporation) on very short timescales so care needs to be exercised in comparing source measurements with ambient measurements for particle size. Also, is it possible that the bimodal ambient measurements are influenced by nucleation rather than exhibiting a vehicle signature?

Response: We thank the referee for pointing out this. We agree that the particles emitted from tailpipe vary substantially in the atmosphere, and the bimodal particle distributions resolved from ambient aerosol cannot link with the particle distribution in the vehicle exhaust directly. So that sentence is deleted in the manuscript.

17. Line 212-214: It would be better to see a description of the correction for dilution, particle, and vapor wall-losses in the methods section.

Response: Thanks for the suggestion. The details of wall-loss correction as well as particle and gas dilution corrections are added in the Supplement.

18. Line 226-229: Zhao et al. (2017) argued that some of the differences in SOA formation between the vehicles they tested could be explained by differences in the NOx levels. Is it possible that differences could be explained by different NOx levels?

Response: Thanks for the suggestion. Zhao et al. reported that ratio of VOCs to NOx has a complex relationship with SOA formation, which is nonmonotonic (Zhao et al., 2017). It could support the discussion in this study.
The sentence has been revised as: "The variation of the SOA production among these studies might be caused by several factors: the model years of vehicles (corresponding to emission standards) (Nordin et al., 2013; Liu et al., 2015), their driving cycles (Nordin et al., 2013), the initial concentrations of gaseous pollutants in the chamber (Jathar et al., 2014), and the ratio of VOCs to NOx (Zhao et al., 2017) in the chamber experiments" between Line 238 to Line 242.

19. Line 239: Explain what underestimated here means?

Response: The loss of semi-volatile vapor deposed to the chamber wall is not calculated, leading to underestimation of SOA production in the chamber experiment.

20. Line 252: Yang et al. (2017) recently suggested that ozonolysis of alkenes in gasoline exhaust could form SOA through aldol condensation reactions. Perhaps cite that study here?

Response: Thanks for your advice. Some discussions on alkenes forming SOA are added between Line 263 to Line 266:

"A recent study found that ozonolysis of alkenes from gasoline vehicle exhaust could form SOA through aldol condensation reactions (Yang et al., 2018). However, much low declines of concentrations were observed than those of aromatics during chamber experiments, so alkenes might not play significant role in SOA formation in this study".

21. Line 255: Units for VOC/NOx ratio? How does this ratio compare to those in megacities?

Response: Thanks for your advice. The unit for VOC/NOx ratio is ppbC/ppb, and modified in the manuscript.
Previous studies revealed that the VOC/NOx ratios were 2.2-9.6 ppbC/ppb for Tianjin (Liu et al., 2016) and 4.3-14.1 ppbC/ppb for Guangzhou (Zou et al., 2015). The ratio in this study is close to the level of high NOx condition in megacities in China.

22. Line 258: Figure 7 shows SOA measurements that are not corrected for vapor wall losses but presumably the SOA mass yields for the aromatic precursors include the effects of vapor wall losses. What is the implication of this? Discuss here.

Response: Thanks. Because the measured SOAs are not corrected for deposition of vapors on the walls, the predicted SOAs calculated by speciated single-ring aromatics including the wall loss vapor lead to overestimation of ratio of predicted SOAs to measured SOAs, indicating that the unspeciated precursors, such as IVOCs and SVOCs, might play a more important role in SOA formation from gasoline vehicle exhaust.

23. Line 264-271: Did the authors consider the detailed speciation data of Zhao et al. (2016) to model the SOA formation from S/IVOCs? Can S/IVOCs explain the unexplained SOA?

Response: Thanks for the suggestion. Zhao et al. reported that the IVOCs accounted for only 4% of NMHC emitted from gasoline vehicles, but they contributed a lot to SOA formation, as much or more than single-ring aromatics. It is a strong support to our study, and it is cited in the Line 283.

24. Line 272-276: My reading of Saliba et al. (2017) (and even May et al. (2014)) is that they do not find any differences in speciation between GDI and PFI vehicles (aromatics versus S/IVOCs) where this work does see differences in SOA production, which it then attributes to differences emissions of aromatics versus S/IVOCs. Elaborate on this discrepancy.

Response: Thanks for the suggestion. The discrepancy might be caused by following reasons: First, some S/IVOCs categories are not measured in the studies of Saliba et al. (2017) and May et al.

(2014), such as long branched and cyclic alkanes. Second, the vehicle-to-vehicle variability and fuel discrepancy might lead to difference in NMOG emissions. And the limited vehicles tested in this studies might also result in uncertainty. More vehicles will be tested and S/IVOC measurement will be included in our future studies.

25. Line 294: GDI vehicles are 25% of the on-road vehicle stock or new vehicle sales?

Response: We thank the reviewer for reminding this. The 25% refers to market share of GDI vehicles in sales. Modified as suggested.

26. Figure 2: Can you add more detail to the caption? What instrument are these data from? Are these from the CVS or chamber? Are these time-averaged? Are the particles denuded?

Response: Thanks for the advice. One sentence is added between Line 543 to Line 544: "The results are average of particle number emissions from vehicles during a whole BJC, measured by DMS500 in the CVS system. The particles were heated to 150℃ in the DMS500".

27. Figure 4: There are definitely more PAH studies that can be compared here, e.g., Hays et al. (2017).

Response: Thanks for the advice. The EFs of PAH compounds are added in Table S2. The main contributors to PAHs mass in this study is compared to the reports from study of Schauer et al. (2002) and Hays et al. (2013) between Line 181 to Line 183: "The main contributors to total PAHs mass emitted from gasoline vehicle exhaust in this study, especially from the GDI vehicle exhaust, was similar with the results reported by previous studies (Schauer et al., 2002; Hays et al., 2013)".

28. Figure 5: This figure is misleading and needs to be redone accounting for the right OH exposures for each study since clearly some of the studies had different OH exposures for different vehicles.

Response: We thank the referee for pointing out this. The Figure 5 has been modified as follow:
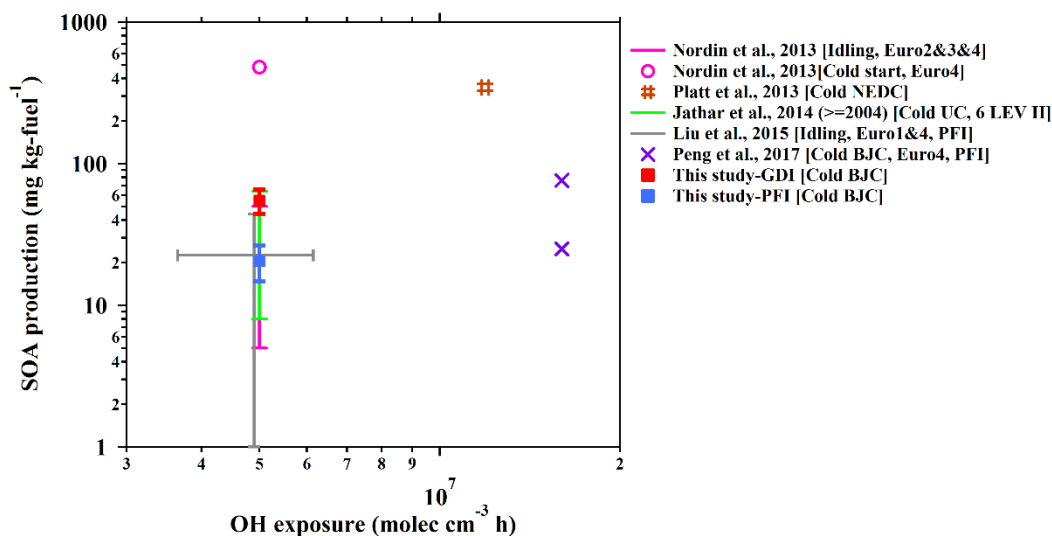
Figure 5. Fuel-based SOA production from gasoline vehicle exhaust as a function of OH exposure in the chamber simulations. The SOA production data are from published studies of chamber simulation of gasoline vehicle exhaust. From the study of Jathar et al. (2014), the SOA production of vehicles manufactured in 2004 or later (LEV II) is selected, which is a model year that is more close to those of the vehicles in this study. The error bars of previous results indicate the range of OH exposure (x axis) and SOA production (y axis) in their simulations. The driving cycles and vehicle information are also noted in the legend of each study.

References:

Alkidas, A. C.: Combustion advancements in gasoline engines, Energy Conversion and Management, 48, 2751-2761, 10.1016/j.enconman.2007.07.027, 2007.

Bahreini, R., Middlebrook, A. M., de Gouw, J. A., Warneke, C., Trainer, M., Brock, C. A., Stark, H., Brown, S. S., Dube, W. P., Gilman, J. B., Hall, K., Holloway, J. S., Kuster, W. C., Perring, A. E., Prevot, A. S. H., Schwarz, J. P., Spackman, J. R., Szidat, S., Wagner, N. L., Weber, R. J., Zotter, P., and Parrish, D. D.: Gasoline emissions dominate over diesel in formation of secondary organic aerosol mass, Geophysical Research Letters, 39, n/a-n/a, 10.1029/2011gl050718, 2012.

Gordon, T. D., Presto, A. A., May, A. A., Nguyen, N. T., Lipsky, E. M., Donahue, N. M., Gutierrez, A., Zhang, M., Maddox, C., Rieger, P., Chattopadhyay, S., Maldonado, H., Maricq, M. M., and Robinson, A. L.: Secondary organic aerosol formation exceeds primary particulate matter emissions for light-duty gasoline vehicles, Atmos. Chem. Phys. , 14, 4661-4678, 10.5194/acp-14-4661-2014, 2014.

Hays, M. D., Preston, W., George, B. J., Schmid, J., Baldauf, R., Snow, R., Robinson, J. R., Long, T., and Faircloth, J.: Carbonaceous aerosols emitted from light-duty vehicles operating on gasoline and ethanol fuel blends, Environmental science & technology, 47, 14502-14509, 10.1021/es403096v, 2013.

Hu, W., Hu, M., Hu, W., Jimenez, J. L., Yuan, B., Chen, W., Wang, M., Wu, Y., Chen, C., Wang, Z., Peng, J., Zeng, L., and Shao, M.: Chemical composition, sources, and aging process of submicron aerosols in Beijing: Contrast between summer and winter, Journal of Geophysical Research-

Atmospheres, 121, 1955-1977, 10.1002/2015jd024020, 2016.

Jathar, S. H., Gordon, T. D., Hennigan, C. J., Pye, H. O. T., Pouliot, G., Adams, P. J., Donahue, N. M., and Robinson, A. L.: Unspeciated organic emissions from combustion sources and their influence on the secondary organic aerosol budget in the United States, Proc. Natl. Acad. Sci. USA, 111, 10473-10478, 10.1073/pnas.1323740111, 2014.

Kanakidou, M., Seinfeld, J. H., Pandis, S. N., Barnes, I., Dentener, F. J., Facchini, M. C., Van Dingenen, R., Ervens, B., Nenes, A., Nielsen, C. J., Swietlicki, E., Putaud, J. P., Balkanski, Y., Fuzzi, S., Horth, J., Moortgat, G. K., Winterhalter, R., Myhre, C. E. L., Tsigaridis, K., Vignati, E., Stephanou, E. G., and Wilson, J.: Organic aerosol and global climate modelling: a review, Atmospheric Chemistry and Physics, 5, 1053-1123, 2005.

Liang, B., Ge, Y., Tan, J., Han, X., Gao, L., Hao, L., Ye, W., and Dai, P.: Comparison of PM emissions from a gasoline direct injected (GDI) vehicle and a port fuel injected (PFI) vehicle measured by electrical low pressure impactor (ELPI) with two fuels: Gasoline and M15 methanol gasoline, Journal of Aerosol Science, 57, 22-31, 10.1016/j.jaerosci.2012.11.008, 2013.

Liu, B., Liang, D., Yang, J., Dai, Q., Bi, X., Feng, Y., Yuan, J., Xiao, Z., Zhang, Y., and Xu, H.: Characterization and source apportionment of volatile organic compounds based on 1-year of observational data in Tianjin, China, Environmental Pollution, 218, 757-769, 10.1016/j.envpol.2016.07.072, 2016.

Myung, C.-L., Kim, J., Choi, K., Hwang, I. G., and Park, S.: Comparative study of engine control strategies for particulate emissions from direct injection light-duty vehicle fueled with gasoline and liquid phase liquefied petroleum gas (LPG), Fuel, 94, 348-355, 10.1016/j.fuel.2011.10.041, 2012.

Saliba, G., Saleh, R., Zhao, Y., Presto, A. A., Lambe, A. T., Frodin, B., Sardar, S., Maldonado, H., Maddox, C., May, A. A., Drozd, G. T., Goldstein, A. H., Russell, L. M., Hagen, F., and Robinson, A. L.: Comparison of Gasoline Direct-Injection (GDI) and Port Fuel Injection (PFI) Vehicle Emissions: Emission Certification Standards, Cold-Start, Secondary Organic Aerosol Formation Potential, and Potential Climate Impacts, Environmental science & technology, 51, 6542-6552, 10.1021/acs.est.6b06509, 2017.

Schauer, J. J., Kleeman, M. J., Cass, G. R. and Simoneit, B. R. T.: Measurement of Emissions from Air Pollution Sources. 5. C1-C32 Organic Compounds from Gasoline-Powered Motor Vehicles, Environmental science & technology, 36, 1169-1180, 2002.

Wen, Y., Wang, Y., Fu, C., Deng, W., Zhan, Z., Tang, Y., Li, X., Ding, H., and Shuai, S.: The Impact of Injector Deposits on Spray and Particulate Emission of Advanced Gasoline Direct Injection Vehicle, SAE Technical Paper, 2016-01-2284, 10.4271/2016-01-2284, 2016.

Yang, B., Ma, P. K., Shu, J. N., Zhang, P., Huang, J. Y. and Zhang, H. X.: Formation mechanism of secondary organic aerosol from ozonolysis of gasoline vehicle exhaust, Environmental Pollution, 234, 960-968, 10.1016/j.envpol.2017.12.048, 2018.

Zhang, Q., Jimenez, J. L., Canagaratna, M. R., Allan, J. D., Coe, H., Ulbrich, I., Alfarra, M. R., Takami, A., Middlebrook, A. M., Sun, Y. L., Dzepina, K., Dunlea, E., Docherty, K., DeCarlo, P. F., Salcedo, D., Onasch, T., Jayne, J. T., Miyoshi, T., Shimono, A., Hatakeyama, S., Takegawa, N., Kondo, Y., Schneider, J., Drewnick, F., Borrmann, S., Weimer, S., Demerjian, K., Williams, P., Bower, K., Bahreini, R., Cottrell, L., Griffin, R. J., Rautiainen, J., Sun, J. Y., Zhang, Y. M., and Worsnop, D. R.: Ubiquity and dominance of oxygenated species in organic aerosols in anthropogenically-influenced Northern Hemisphere midlatitudes, Geophysical Research Letters, 34, 10.1029/2007gl029979, 2007.

Zhao, Y., Saleh, R., Saliba, G., Presto, A. A., Gordon, T. D., Drozd, G. T., Goldstein, A. H., Donahue, N. M., and Robinson, A. L.: Reducing secondary organic aerosol formation from gasoline vehicle exhaust, Proceedings of the National Academy of Sciences of the United States of America, 114, 6984-6989, 10.1073/pnas.1620911114, 2017.

Zimmerman, N., Wang, J. M., Jeong, C.-H., Ramos, M., Hilker, N., Healy, R. M., Sabaliauskas, K., Wallace, J. S., and Evans, G. J.: Field Measurements of Gasoline Direct Injection Emission Factors: Spatial and Seasonal Variability, Environmental science & technology, 50, 2035-2043, 10.1021/acs.est.5b04444, 2016.

Zou, Y., Deng, X. J., Zhu, D., Gong, D. C., Wang, H., Li, F., Tan, H. B., Deng, T., Mai, B. R., Liu, X. T., and Wang, B. G.: Characteristics of 1 year of observational data of VOCs, NOx and O-3 at a suburban site in Guangzhou, China, Atmospheric Chemistry and Physics, 15, 6625-6636, 10.5194/acp-15-6625-2015, 2015.

Comparison of primary aerosol emission and secondary aerosol formation from gasoline direct injection and port fuel injection vehicles

Zhuofei Du[1], Min Hu[1, 3*], Jianfei Peng[1†], Wenbin Zhang[2], Jing Zheng[1], Fangting Gu[1], Yanhong Qin[1], Yudong Yang[1], Mengren Li[1], Yusheng Wu[1], Min Shao[1], Shijin Shuai[2]

1. State Key Joint Laboratory of Environmental Simulation and Pollution Control, College of Environmental Sciences and Engineering, Peking University, Beijing 100871, China

2. State Key Laboratory of Automotive Safety and Energy, Department of Automotive Engineering, Tsinghua University, Beijing 100084, China

3. Beijing Innovation Center for Engineering Sciences and Advanced Technology, Peking University, Beijing 100871, China

[†] Now at Department of Atmospheric Sciences, Texas A&M University, College Station, TX 77843, US

*Corresponding author: Min Hu, minhu@pku.edu.cn

Abstract

Gasoline vehicles greatly contribute to urban particulate matter (PM) pollution. Gasoline direct injection (GDI) engines, known as their higher fuel efficiency than that of port fuel injection (PFI) engines, have been increasingly employed in new gasoline vehicles. However, the impact of this trend on air quality is still poorly understood. Here, we investigated both primary emissions and secondary organic aerosol (SOA) formation from GDI and PFI vehicles under urban-like condition, using combined approaches involving chassis dynamometer measurement and environmental chamber simulation. The PFI vehicle emits slightly more volatile organic compounds, e.g., benzene and toluene, whereas the GDI vehicle emits more particulate components, e.g., the total PM, elemental carbon, primary organic aerosols and polycyclic aromatic hydrocarbons. Strikingly, a much higher SOA production (by a factor of approximately 2.7) is found from the exhaust of the GDI vehicle than that of the PFI vehicle under the

same conditions. More importantly, the higher SOA production found in the GDI vehicle exhaust occurs concurrently with lower concentrations of traditional SOA precursors, e.g., benzene and toluene, indicating a greater contribution of intermediate volatility organic compounds and semivolatile organic compounds in the GDI vehicle exhaust to the SOA formation. Our results highlight the considerable potential contribution of GDI vehicles to urban air pollution in the future.

1 Introduction

Organic aerosols account for approximately 20-50 % of ambient fine particulate matter ($PM_{2.5}$), with significant environment and health effects (Kanakidou et al., 2005). Primary organic aerosol (POA) is emitted directly by sources, while secondary organic aerosol (SOA) is mainly formed via oxidation of gaseous precursors in the atmosphere and account for about 30-90 % of the organic aerosol (OA) mass worldwide (Zhang et al., 2007; Hu et al., 2016), but SOA source remain poorly constrained. Robinson et al. (2007) proposed that low-volatility gas-phase species emitted from diesel vehicles were important sources for urban ambient SOA, which achieved better mass closure between observed and modeled SOA. Using an updated CMAQ model, Jathar et al. (2017) found that 30-40% OA was contributed from vehicles in the southern California, and half of which was SOA. Huang et al. (2014) recently revealed that 15-65 % of SOA was contributed by fossil fuel consumption (i.e., traffic and coal burning) in megacities in China. These indicated that vehicles have important contribution to ambient SOA in urban areas. An ambient organic aerosol measurement in the Los Angeles Basin demonstrated that SOA contributed from gasoline vehicles was significant in the urban air, much larger than that from diesel vehicles (Bahreini et al., 2012). Similar conclusion was reached by Hayes et al. (2013) based on mass spectrometer results. Meanwhile, several chamber simulation studies concluded that exhaust of gasoline vehicles could form substantial SOA (Jathar et al., 2014). Thus, gasoline vehicles exhaust is highly associated with ambient SOA formation.

Gasoline vehicles can be categorized into two types based on the fuel injection technologies in their engines, i.e., port fuel injection (PFI) vehicles and gasoline direct injection (GDI) vehicles. Unlike a PFI engine, in which

gasoline is injected into intake port, gasoline is sprayed into cylinder directly in a GDI engine. With the increased atomization and vaporization rate of fuel, and more accurate control of fuel volume and injection time, a GDI engine has many advantages, such as better fuel efficiency, lower CO_2 emissions and less fuel pumping loss (Alkidas, 2007; Myung et al., 2012; Liang et al., 2013). In past decades, PFI vehicles dominated the market share of gasoline cars in the world. However, in recent years, GDI vehicles have been increasingly employed, due to their higher fuel efficiency. The market share of GDI vehicles in sales in 2016 reached about 25 %, 50 % and 60 % in China, the US and Europe, respectively (Wen et al., 2016; Zimmerman et al., 2016).

Several previous studies investigated the emissions of GDI and PFI vehicles, in terms of concentrations of gaseous pollutants, particle numbers and mass concentrations, and evaluated the reduction of emissions with the upgrading emission standards (Ueberall et al., 2015; Zhu et al., 2016; Saliba et al., 2017). These studies show that GDI vehicles emit more primary particles than PFI vehicles (Zhu et al., 2016; Saliba et al., 2017), and even diesel vehicles equipped with diesel particulate filter (DPF) (Wang et al., 2016), which is likely due to insufficient time allowed for gasoline fuel to be mixed with air thoroughly, as well as gasoline droplets impinging onto pistons and surfaces of combustion chamber in GDI engine (Chen et al., 2017; Fu et al., 2017). However, in most studies, vehicles were tested under the driving cycles of the US or European standards, indicating that those results are not representative of China's traffic conditions.

SOA production from gasoline vehicle exhaust was previously simulated in smog chambers and potential aerosol mass (PAM) flow reactors. SOA formed from gaseous pollutants exceeds the related POA emissions and having much more contribution to air quality degradation. These studies mostly focused on the impacts of SOA formation by the model year (Gordon et al., 2014; Jathar et al., 2014; Liu et al., 2015), fuel formulations (Peng et al., 2017), driving cycles (including idling) (Nordin et al., 2013; Platt et al., 2013) and start-up modes of the gasoline vehicles (Nordin et al., 2013). Few studies, however, have investigated SOA formation from vehicles with different engine technologies (GDI and PFI) under the same working condition.

In this study, both primary emissions and secondary aerosol formation from GDI and PFI vehicles were investigated. To represent typical urban driving patterns in megacities such as Beijing, the vehicles were tested

76 using gasoline fuel meeting the China Phase V fuel standard, and were operated with the cold-start Beijing cycle

77 (BJC). The SOA formation from both the PFI and GDI vehicle exhausts were then simulated using a smog chamber.

78 Finally, the overall contributions of the GDI and PFI gasoline vehicles to ambient particulate matter (PM) were

79 evaluated. This study is part of a project that investigates the relationship between vehicle (engine) emissions and

80 ambient aerosols, including potential of SOA formation from a PFI engine (Du et al., 2017) and the effects of

81 gasoline aromatics on SOA formation (Peng et al., 2017).

82

83 **2 Materials and methods**

84 **2.1 Vehicles**

85 One PFI vehicle and one GDI vehicle were tested in this study to investigate their primary emissions and SOA

86 formations. In this study, the selected PFI and GDI vehicles were certified to the China Phase IV Emissions

87 Standard (equivalent to Euro IV) and the China Phase V Emissions Standard (equivalent to Euro V), respectively.

88 More information of the vehicles is shown in Table 1. The fuel used in the experiments was a typical Phase V

89 gasoline on the China market (sulfur content = 6 mg kg^{-1}). More information of the fuel is provided in Table S1 in

90 the Supplement. Cold-start BJC, characterized by a higher proportion of idling periods and lower acceleration

91 speeds than the New European Driving Cycle (NEDC), was performed to simulate the repeated braking and

92 acceleration on road in megacities such as Beijing. The BJC lasted approximately 17 minutes, with a maximum

93 speed of 50 km h^{-1} (Peng et al., 2017).

94

95 **2.2 Experimental setup**

96 The chamber experiments were carried out in the summer at the State Key Laboratory of Automotive Safety

97 and Energy of Tsinghua University in Beijing, including two experiments conducted with GDI vehicle and four

98 experiments conducted with PFI vehicle. The tested vehicles were placed on a chassis dynamometer system (Burke

99 E. Porter Machinery Company) with a controlled room temperature and absolute humidity of 26.4±2.5 ℃ and

100 11.5±2.4 g m^{-3}, respectively. The exhaust emitted by the vehicle tailpipe was diluted in a constant volume sampler

101 (CVS) system, where the flow was maintained at 5.5 m^3 min^{-1} using filtered ambient air, achieving about 20 times

102 dilution of the exhaust. Several instruments, including an AVL CEBII gas analyzer, a Cambustion Differential

103 Mobility Spectrometer (DMS500) and a particle sampler, were connected to the CVS (detailed in Figure 1 and

104 section 2.3) to characterize the primary gas- and particulate-phase pollutants. The diluted exhausts produced by the

105 CVS system were injected into an outdoor chamber, where secondary aerosol formation from gasoline vehicle

106 exhausts was simulated. This was the second dilution step of the exhausts and had a dilution factor of approximately

107 15. A schematic illustration of the outdoor experimental setup is shown in Figure 1.

108   The photochemical oxidation experiments were carried out in a quasi-atmospheric aerosol evolution study

109 (QUALITY) outdoor chamber. More details of the setup and performance of the QUALITY chamber were

110 introduced by Peng et al. (2017). Prior to each experiment, the chamber was covered with a double-layer anti-

111 ultraviolet (anti-UV) shade to block sunlight and was cleaned with zero air for about 15 h to create a clean

112 environment. Approximately 120 ppb O_3 were injected into the chamber prior to the injection of vehicle exhaust to

113 make the oxidation environment similar to the mean O_3 peak concentration in the ambient atmosphere. Before the

114 chamber was exposed to sunlight, about 15-minute period was left to ensure that the pollutants mixed sufficiently

115 in the chamber, then the initial concentrations were characterized in the dark. Subsequently, the anti-UV shade

116 were removed from the chamber and photo-oxidation was initiated. A suite of high time resolution instruments was

117 utilized to track the evolution of pollutants during the chamber experiments. Zero air was added into the chamber

118 when sampling to maintain a constant pressure.

119

120 **2.3 Instrumentation**

121   Primary gases and aerosols were measured by the instruments connected to the CVS. The concentrations of

122 gaseous pollutants, including CO, CO_2, NO_x and total hydrocarbon (THC) were monitored with a gas analyzer

123 AVL Combustion Emissions Bench II (CEB II, AVL, Austria). Primary aerosols were measured with both on-line

124 and off-line instruments. A DMS500 (Cambustion, UK) was implemented to monitor the real-time number size

125 distribution and total number concentration of primary particles. Its sampling line was heated to maintain the

126 temperature at 150℃. The aerosols were also collected on Teflon and quartz filters by AVL Particulate Sampling

127 System (SPC472, AVL, Austria) to analyze the mass, organic carbon (OC) and elemental carbon (EC) emission

128 factors using a balance and OC/EC analyzer (Sunset Lab, USA).

129   During the chamber experiments, a suite of real-time instruments was utilized to characterize the evolutions

130 of the gas and particulate-phase pollutants. CO analyzer, NO-NO_2-NO_x analyzer and O_3 analyzer (Thermo Fisher

131 Scientific Inc., USA) were employed to measure the concentrations of CO, NO_x (including NO and NO_2) and O_3,

132 respectively. The evolutions of volatile organic compounds (VOCs) were monitored with a proton transfer reaction

133 mass spectrometer (PTR-MS, IoniconAnalytik, Austria) (Lindinger et al., 1998). H_3O^+ was used as the reagent ion,

134 which reacted with the target compounds. The resulting ions were detected by a quadruple mass spectrometer.

135 Meanwhile, the particles size distribution was characterized using a scanning mobility particle sizer system (SMPS,

136 TSI, USA), which consisted of a differential mobility analyzer (DMA, TSI, USA) and a condensation particle

137 counter (CPC, TSI, USA). This system can measure aerosols with a diameters ranging from 15 nm to 700 nm. A

138 high-resolution time-of-flight aerosol mass spectrometer (HR-Tof-AMS, Aerodyne Research, USA) was applied to

139 obtain mass concentrations and size distributions of submicron, non-refractory aerosols, including sulfate, nitrate,

140 ammonium, chloride and organic (DeCarlo et al., 2006). Table 2 lists the instruments used to measure the primary

141 emissions and their evolutions in the chamber experiments.

142

143 **3 Results**

144 **3.1 Primary emissions**

145 **Gaseous pollutant emissions**

146   Emission factors (EFs) of CO_2, THC, benzene and toluene from the GDI and PFI vehicles are listed in Table

147 3. The EFs of CO_2 and THC are derived from measured concentrations in CVS, while the EFs of benzene and

148 toluene were calculated from the initial concentrations in the chamber. The THC emission factor was reported in

149 units of carbon mass, g C kg^{-1}fuel^{-1}.

150   The GDI vehicle emitted less CO_2 and THC than the PFI vehicle due to their different fuel injection strategies

151   and mixing features (Liang et al. 2013; Gao et al., 2015). The EF of THC from the GDI vehicle met the standard

152   of the China Phase V Emission Standard (0.1 g km^{-1}), but that from the PFI vehicle was slightly beyond the standard

153   limit. The PFI vehicle used in this study met lower emission standard (the China Phase IV), which might cause

154   additional THC emission when compared to the China Phase V Emission Standard. In addition, BJC and NEDC

155   were applied in this study and emission standard, respectively. More repeated braking and acceleration in BJC

156   might cause incomplete combustion and consequently higher THC emission from the PFI vehicle in this study. As

157   typical VOC species emitted by vehicles, benzene and toluene were measured in this study. For both vehicles, the

158   EFs of toluene were higher than those of benzene. Consistent with the feature of THC emission, the PFI vehicle

159   emitted more benzene and toluene than the GDI vehicle, and the enhancement of toluene was much larger than that

160   of benzene.

161   The EFs of the gaseous pollutants in this study had similar magnitudes to those in previous studies in which

162   gasoline vehicles met comparable levels of emission standards and were tested under cold-start driving condition,

163   while the results in this study were slightly higher, as shown in Table 3. This difference might be because the

164   California ultralow-emission vehicles (ULEV) (Saliba et al., 2017) and most LEV II vehicles (manufactured in

165   2004 or later) (May et al., 2014) meet the US certification gasoline emission standards for the ULEV category,

166   which has a lower limit of gaseous pollutants than the China Phase V Emission Standard. In addition, the different

167   driving cycles of our study and those other studies (listed in Table 3) might be another explanation for the difference

168   in the EFs of gaseous pollutants.

169   **Primary particle emissions**

170   The EFs of PM, elemental carbon (EC), POA and particulate polycyclic aromatic hydrocarbons (PAHs) are

171   shown in Table 4. The EF of PM$_{2.5}$ from the GDI vehicle was about 1.4 times higher than that of the PFI vehicle.

172   Both vehicles met the China Phase V Emission Standard for PM emission (4.5 mg km^{-1}). The GDI vehicle emitted

173   about 3.3 times more EC and 1.2 times more POA than the PFI vehicle. The primary carbonaceous aerosols

174   (EC+POA) accounted for 85 % and 82 % of the PM in the GDI and PFI vehicles respectively, suggesting that

175   carbonaceous aerosols were the major contributors in the PM from gasoline vehicles, especially for the GDI vehicle.

176   PAHs account for a small fraction of particulate organic matter in the atmosphere, but the molecular signature

177   of PAHs can be utilized in source identification of vehicle emissions (Kamal et al., 2015). The GDI vehicle emitted

178   about 1.5 times the PAHs of the PFI vehicle. The EFs of PAH compounds are listed in Table S2 in the Supplement,

179   and details of PAHs measurement was described in Li et al. (2016). It should be noted that the PAHs were tested

180   under warm-start cycles. A higher EF of PAHs would be obtained under cold-start cycle, since the lower

181   temperature led to inefficient catalyst at the beginning of cold-start (Mathis et al., 2005). The main contributors to

182   total PAHs mass emitted from gasoline vehicle exhaust in this study, especially from the GDI vehicle exhaust, was

183   similar with the results reported by previous studies (Schauer et al., 2002; Hays et al., 2013).

184   The lower $PM_{2.5}$ and POA emissions from GDI vehicle were found in previous studies, except that a little

185   higher $PM_{2.5}$ emission from GDI vehicle was illustrated in Saliba's study (Platt et al., 2013; May et al., 2014; Zhu

186   et al., 2016; Saliba et al., 2017). The EC emissions were in the range of those of previous studies but on the lower

187   level. The EF of the POA measured in this study was higher than those of other studies, leading to a higher OC/EC

188   ratio, which could be attributed to the less strict emission standard of our vehicles and the different driving cycles

189   applied in the experiments.

190   The bimodal number size distributions of the primary PM from the vehicles measured by the DMS500 are

191   shown in Figure 2. The particle distributions of the exhausts of the GDI and PFI vehicles illustrated similar patterns,

192   with two peaks located at about 10 nm for nucleation mode and at 60-90 nm for accumulation mode, respectively,

193   which are consistent with the results of previous studies (Maricq et al., 1999; Chen et al., 2017). The particle

194   number size distribution of the exhausts of the GDI vehicle showed a similar pattern to that of the PFI vehicle, with

195   a much higher number concentration that is consistent with the emission of more particle mass.

196

197   **3.2 SOA formation from gasoline vehicle exhaust**

198   The time-resolved concentrations of gases and particles during the chamber experiments are illustrated in

199   Figure 3. Before removing the anti-UV shade, the initial concentrations of NO_x, benzene and toluene from the PFI

200   and GDI vehicles were 80 ppb, 3 ppb, 5 ppb and 100 ppb, 4 ppb, 14 ppb respectively.

201   After the aging experiment started (t=0 in Figure 3), NO was formed from NO_2 photolysis, and then reacted

202   with O_3 to form NO_2. The O_3 concentration increased rapidly to a maximum within 2-3 h and then decreased via

203   reactions and dilution. Benzene and toluene decayed during the aging process at different rates.

204   New particle formation was found inside the chamber 15 minutes after the exhaust was exposed to sunlight,

205   providing substantial seeds for secondary aerosol formation. Significant growths of particles in both size and mass

206   were observed in the chamber, indicating that a large amount of secondary aerosol was formed during the

207   photochemical oxidation. The chemical compositions of the secondary aerosols were measured continuously by

208   HR-Tof-AMS. Organic was the dominant composition of the secondary aerosol, accounting for 88-95 % of the

209   total particle mass inside the chamber (Figure S1), which is consistent with our previous research (Peng et al.,

210   2017). The SOA mass exhibited different growth rate for the two types of vehicles. After a 4 h oxidation in the

211   chamber, the SOA formed from the exhaust of the GDI vehicle was approximately double that of the PFI vehicle.

212   The solar radiation conditions significantly influenced the SOA formation. Thus, OH exposure was used to

213   characterize the photochemical age as a normalization, instead of the experiment time. Two VOC species with

214   noticeable differences in their reaction rate constants with OH radicals could be utilized to calculate the OH

215   exposure ([OH] Δt) based on Equation 1 (for benzene and toluene, as used in this study) (Yuan et al., 2012).

216    $[OH] \Delta t = \frac{1}{k_T - k_B} \times \left(\ln \frac{[T]}{[B]} \Big|_{t=0} - \ln \frac{[T\}}{[B]} \right)$ (1)

217   where k_T and k_B are the OH rate constants of benzene (1.2×10^{-12} cm^3 molecule^{-1} s^{-1}) (Yuan et al., 2012) and toluene

218   (5.5×10^{-12} cm^3 molecule^{-1} s^{-1}) (Kramp and Paulson, 1998), respectively. $\frac{[T]}{[B]} \Big|_{t=0}$ is the concentration ratio of

219   toluene to benzene at the beginning of the aging process, and $\frac{[T]}{[B]}$ is their concentration ratio measured during

220   aging process.

221   The SOA concentrations as a function of OH exposure are illustrated in Figure 4. Wall-loss correction and

222   dilution correction, including both particles and gaseous pollutants, were taken into consideration in the calculation

223   of the SOA mass concentration in the chamber. Detailed descriptions of corrections are given in the Supplement.

224   Assuming the mean OH concentration was 1.6×10^6 molecular cm^{-3} in Beijing (Lu et al., 2013), the whole aging

225 procedure in the chamber experiments was equal to a 6-10 h atmospheric photochemical oxidation. The average

226 SOA concentrations were 9.25±1.80 and 4.68±1.32 μg m^{-3} for the GDI and PFI vehicles, respectively, when the

227 OH exposure was 5×10^6 molecular cm^{-3} h in the chamber. Considering the driving cycle mileage and fuel

228 consumption, the SOA productions were 54.77±10.70 mg kg-fuel^{-1} or 3.06±0.60 mg km^{-1} for the GDI vehicle and

229 20.57±5.82 mg kg-fuel^{-1} or 1.55±0.44 mg km^{-1} for the PFI vehicle. Compared with the PFI vehicle, the GDI vehicle

230 exhaust exhibited a higher potential of SOA formation, even though the PFI vehicle emitted more VOCs, which

231 are considered as dominant class of SOA precursors. This result indicates that higher concentrations of some other

232 SOA precursors exist in the exhaust of GDI vehicles, which will be further discussed in section 3.3.

233 The results from chamber simulation of SOA formation from individual gasoline vehicles are illustrated in

234 Figure 5. The SOA production from the both vehicles in this study is in the range of the results of previous studies

235 (Nordin et al., 2013; Platt et al., 2013; Jathar et al., 2014; Liu et al., 2015; Peng et al., 2017). The variation of the

236 SOA production among these studies might be caused by several factors: the model years of vehicles

237 (corresponding to emission standards) (Nordin et al., 2013; Liu et al., 2015), their driving cycles (Nordin et al.,

238 2013), the initial concentrations of gaseous pollutants in the chamber (Jathar et al., 2014), and the ratio of VOCs to

239 NO$_x$ (Zhao et al., 2017) in the chamber experiments.

240 To investigate the dominant contributors to ambient PM from the GDI and PFI vehicles, Figure 6 illustrates

241 the EFs of EC and POA as well as the production factors of SOA in this study. The SOA production from the GDI

242 vehicle was approximately 2.7 times higher than that from the PFI vehicle. At 5×10^6 molecular cm^{-3} h OH exposure,

243 the SOA/POA ratio was approximately 1. Figure 4 illustrates that the SOA production increased with

244 photochemical age rapidly (within 2×10^7 molecular cm^{-3} h). Thus, SOA would exceed POA at higher OH exposure,

245 e.g., the SOA/POA ratio reached about 4 at 10^7 molecular cm^{-3} h OH exposure, becoming the major PM contributor.

246 In terms of the POA and EC emissions as well as the SOA formation, the GDI vehicle contributed 2.2 times more

247 than the PFI vehicle.

248 Although particle wall-loss correction as well as particle and gas dilution corrections were considered in this

249 study, several factors may still contribute to the uncertainties of the SOA productions. First, the deposition of semi-

10

250 volatile vapors to the chamber walls was not corrected, which may result in an underestimation of the rate of SOA

251 production with a factor of 1.1-4.1 (Zhang et al., 2014). Second, under some ambient conditions such as severe

252 urban haze events (Guo et al., 2014), particle mass concentrations can be as high as 200-300 ug m^{-3}, much higher

253 than the 23 $\pm$6 ug m^{-3} under the chamber condition in this study. High particle mass loadings are favorable for the

254 partition of semi-volatile compounds into the particle phase, potentially increasing the rate of SOA production

255 (Odum et al., 1996). Third, stronger partitioning of SOA precursors into the particle phase may reduce the oxidized

256 products in the gas phase, which will potentially reduce the rate of SOA production (Seinfeld et al., 2003)

257

258 **3.3 SOA mass closure**

259   SOA production ($\Delta OA_{predicted}$) estimated from VOC precursors can be defined as Eq. (2):

260 $\Delta OA_{predicted} = \sum_i (\Delta_i \times Y_i)$ (2)

261 where Δ_i is the concentration change of precursor VOC$_i$ measured with PTR-MS in the chamber experiments, and

262 Y_i is the SOA yield of the VOC$_i$. In this study, benzene, toluene, C8 benzene and C9 benzene were involved in the

263 estimation of SOA production, and alkanes and alkenes were not considered. A recent study found that ozonolysis

264 of alkenes from gasoline vehicle exhaust could form SOA through aldol condensation reactions (Yang et al., 2018).

265 However, much low declines of concentrations were observed than those of aromatics during chamber experiments,

266 so alkenes might not play significant role in SOA formation in this study.

267   The SOA yield is sensitive to VOCs/NO$_x$ ratio (Song et al., 2005). In this study, the VOCs/NO$_x$ ratio was in

268 the range of 0.5-1.0 ppbC/ppb, thus, the SOA formation from the vehicle exhaust was determined under high NO$_x$

269 conditions. The high NO$_x$ SOA yields of benzene and toluene were taken from Ng et al. (2007). The C8 and C9

270 benzene used the SOA yield of m-xylene from Platt et al. (2013).

271   The increased predicted SOA contribution from the VOC precursors as a function of OH exposure

272 accumulation is demonstrated in Figure 7. At the end of the experiments, the SOA estimated from these speciated

273 VOCs accounted for about 25 % and 53 % of the measured SOA formation from the GDI and PFI vehicle exhausts,

274 respectively. Similar to the results of previous studies (Platt et al., 2013; Nordin et al., 2013; Gordon et al., 2014),

single-ring aromatics played an important role in the SOA formation, especially for the PFI vehicle which shows higher predicted SOA fraction.

The unpredicted fraction of the measured SOA in the chamber experiments was in the range of 47-75 %. Contributions from intermediate volatility organic compounds (IVOCs) and semivolatile organic compounds (SVOCs), e.g., long branched and cyclic alkanes and gas-phase polycyclic aromatic hydrocarbons could be a possible explanation for this underestimation. The SOA formed by oxidation of IVOCs and SVOCs is found to dominate over that from single-ring aromatics (Robinson et al., 2007; Zhao et al., 2016). The unpredicted SOA ratio exhibited a maximum value at the beginning of the experiment, indicating that the IVOCs and SVOCs with low volatilities produced SOA much more efficiently than the single-ring aromatics with high volatilities, as the first generation products of photo-oxidation of these precursors form SOA (Robinson et al., 2007).

The larger fraction of the unpredicted SOA from the GDI vehicle exhaust might be associated with higher IVOCs and SVOCs emissions. Gas-phase PAH is one of the main component of speciated IVOCs (Zhao et al., 2016). The particulate-phase PAHs from the GDI vehicle were more abundant than those from the PFI vehicle by a factor of 1.5 (section 3.1). Based on gas-particle equilibrium, this indicates that more gas-phase PAHs, including some aromatic IVOCs, might be emitted by the GDI vehicles, contributing to the SOA enhancement.

4 Discussions and conclusions

GDI and PFI vehicles have different fuel injection technologies in their engines, which affects their emissions of gaseous and particulate pollutants. In GDI engine, the fuel is directly injected into cylinder, which benefits the fuel atomization and vaporization and provides better control of fuel volume and the combustion process (Liang et al. 2013; Gao et al., 2015). Thus, in this study, the tested GDI vehicle has higher fuel economy and lower THC emission than the PFI vehicle. However, the insufficient mixing time allowed for the fuel and air leads to incomplete combustion in the GDI engine (Fu et al., 2014). In addition, direct fuel injection leads to fuel impingement onto surfaces of combustion chamber, where liquid pools form, favoring soot-like particulate formation (Ueberall et al., 2015; Chen et al., 2017). Consequently, larger particle mass and number are emitted by

300   the GDI vehicle than from the PFI vehicle. The particles emitted by the GDI vehicle have higher EC mass fraction,

301   leading to lower OC/EC ratio. The considerable particle number emitted by gasoline vehicles, especially in GDI

302   vehicles exhaust, makes a significant contribution to particle number concentration as well as seeds for further

303   reactions in the atmosphere, and needs to be controlled in the future emission standards.

304   Our results show that the GDI vehicle contributes more to both primary and secondary aerosol than the PFI

305   vehicle, and has greater impact on environment and air quality. In recent years, the market share of GDI vehicles

306   exerts a continuous growth in China because they provide better fuel economy and lower CO_2 emissions. In 2016,

307   GDI vehicles accounted for 25 % of China's market share in sales, and this proportion is expected to reach 60 %

308   by 2020 (Wen et al., 2016). The PM enhancement of GDI vehicles with increasing population could potentially

309   offset any PM emission reduction benefits, including the development of gasoline emission and fuel standards and

310   the advanced engine technologies of gasoline vehicles. Therefore, our results highlight the necessity of further

311   research and regulation of GDI vehicles.

312   It should be pointed out that the SOA formation factors in this study are based on one GDI vehicle and one

313   PFI vehicle. Some previous studies proposed that vehicles have variations even though they meet similar

314   specification vehicles and use the same fuel (Gordon et al., 2014; Jathar et al., 2014). Thus more researches with

315   more vehicles for each technology are needed on SOA formation from vehicle exhaust.

316   Primary emissions and secondary organic formation from one GDI vehicle and one PFI vehicle were

317   investigated when driving under cold-start BJC. The primary PM emitted by the GDI vehicle was 1.4 times greater

318   than that from the PFI vehicle and the SOA formation from the GDI vehicle exhaust was 2.7 times greater than that

319   from the PFI vehicle exhaust for the same OH exposure. The SOA production factors were 54.77 ± 10.70 mg kg-

320   fuel^{-1} or 3.06 ± 0.60 mg km^{-1} for the GDI vehicle and 20.57 ± 5.82 mg kg-fuel^{-1} or 1.55 ± 0.44 mg km^{-1} for the PFI

321   vehicle at an OH exposure of 5×10^6 molecular cm^{-3} h, which is consistent with the values seen in previous studies.

322   Considering the higher amounts of OA derived from primary emission and secondary formation, the GDI vehicle

323   contribute considerably more to particle mass concentrations in the ambient air than the PFI vehicle.

324   The SOA formation was predicted from the gaseous precursors emitted by the GDI and PFI vehicles under

325 high NO$_x$ condition. Single-ring aromatic VOCs could explain only 25-53 % of the measured SOA formation in

326 the chamber experiments. The GDI vehicle exhibited higher fraction of unexplained SOA. More IVOCs and

327 SVOCs were inferred as being emitted by the GDI vehicle.

328 With increasing population of GDI vehicles, any benefits of the aerosol emission reduction of gasoline

329 vehicles are substantially offset, because GDI vehicles have significant contributions to ambient aerosols. More

330 work is needed to improve the understanding of GDI vehicle emissions and to provide information for the

331 regulation of gasoline vehicles.

332

333

334 *Data availability*. The data presented in this article are available from the authors upon request

335 (minhu@pku.edu.cn).

336

337

344

345 **Reference**

346 Alkidas, A. C.: Combustion advancements in gasoline engines, Energy Conversion and Management, 48, 2751-

347 2761, 10.1016/j.enconman.2007.07.027, 2007.

348 Bahreini, R., Middlebrook, A. M., de Gouw, J. A., Warneke, C., Trainer, M., Brock, C. A., Stark, H., Brown, S. S.,

349 Dube, W. P., Gilman, J. B., Hall, K., Holloway, J. S., Kuster, W. C., Perring, A. E., Prevot, A. S. H., Schwarz, J. P.,

350 Spackman, J. R., Szidat, S., Wagner, N. L., Weber, R. J., Zotter, P., and Parrish, D. D.: Gasoline emissions dominate

351 over diesel in formation of secondary organic aerosol mass, Geophysical Research Letters, 39,

352 10.1029/2011gl050718, 2012.

353 Chen, L., Liang, Z., Zhang, X., and Shuai, S.: Characterizing particulate matter emissions from GDI and PFI

354 vehicles under transient and cold start conditions, Fuel, 189, 131-140, 10.1016/j.fuel.2016.10.055, 2017.

355 DeCarlo, P. F., Kimmel, J. R., Trimborn, A., Northway, M. J., Jayne, J. T., Aiken, A. C., Gonin, M., Fuhrer, K.,

356 Horvath, T., Docherty, K. S., Worsnop, D. R., and Jimenez, J. L.: Field-deployable, high-resolution, time-of-flight

357 aerosol mass spectrometer, Analytical Chemistry, 78, 8281-8289, 10.1021/ac061249n, 2006.

358 Du, Z., Hu, M., Peng, J., Guo, S., Zheng, R., Zheng, J., Shang, D., Qin, Y., Niu, H., Li, M., Yang, Y., Lu, S., Wu,

359 Y., Shao, M., and Shuai, S.: Potential of secondary aerosol formation from Chinese gasoline engine exhaust, Journal

360 of environmental sciences, 2017, in press.

361 Fu, H., Wang, Y., Li, X., and Shuai, S.: Impacts of Cold-Start and Gasoline RON on Particulate Emission from

362 Vehicles Powered by GDI and PFI Engines, SAE Technical Paper, 2014-01-2836, 10.4271/2014-01-2836, 2014.

363 Gao, Z., Curran, S. J., Parks, J. E., II, Smith, D. E., Wagner, R. M., Daw, C. S., Edwards, K. D., and Thomas, J. F.:

364 Drive cycle simulation of high efficiency combustions on fuel economy and exhaust properties in light-duty

365 vehicles, Applied Energy, 157, 762-776, 10.1016/j.apenergy.2015.03.070, 2015.

366 Gentner, D. R., Jathar, S. H., Gordon, T. D., Bahreini, R., Day, D. A., El Haddad, I., Hayes, P. L., Pieber, S. M.,

367 Platt, S. M., de Gouw, J., Goldstein, A. H., Harley, R. A., Jimenez, J. L., Prevot, A. S. H., and Robinson, A. L.:

368 Review of Urban Secondary Organic Aerosol Formation from Gasoline and Diesel Motor Vehicle Emissions,

369 Environmental science & technology, 51, 1074-1093, 10.1021/acs.est.6b04509, 2017.

Gordon, T. D., Presto, A. A., May, A. A., Nguyen, N. T., Lipsky, E. M., Donahue, N. M., Gutierrez, A., Zhang, M., Maddox, C., Rieger, P., Chattopadhyay, S., Maldonado, H., Maricq, M. M., and Robinson, A. L.: Secondary organic aerosol formation exceeds primary particulate matter emissions for light-duty gasoline vehicles, Atmos. Chem. Phys. , 14, 4661-4678, 10.5194/acp-14-4661-2014, 2014.

Guo, S., Hu, M., Zamora, M. L., Peng, J., Shang, D., Zheng, J., Du, Z., Wu, Z., Shao, M., Zeng, L., Molina, M. J., and Zhang, R.: Elucidating severe urban haze formation in China, Proceedings of the National Academy of Sciences of the United States of America, 111, 17373-17378, 10.1073/pnas.1419604111, 2014.

Hayes, P. L., Ortega, A. M., Cubison, M. J., Froyd, K. D., Zhao, Y., Cliff, S. S., Hu, W. W., Toohey, D. W., Flynn, J. H., Lefer, B. L., Grossberg, N., Alvarez, S., Rappenglueck, B., Taylor, J. W., Allan, J. D., Holloway, J. S., Gilman, J. B., Kuster, W. C., De Gouw, J. A., Massoli, P., Zhang, X., Liu, J., Weber, R. J., Corrigan, A. L., Russell, L. M., Isaacman, G., Worton, D. R., Kreisberg, N. M., Goldstein, A. H., Thalman, R., Waxman, E. M., Volkamer, R., Lin, Y. H., Surratt, J. D., Kleindienst, T. E., Offenberg, J. H., Dusanter, S., Griffith, S., Stevens, P. S., Brioude, J., Angevine, W. M., and Jimenez, J. L.: Organic aerosol composition and sources in Pasadena, California, during the 2010 CalNex campaign, Journal of Geophysical Research-Atmospheres, 118, 9233-9257, 10.1002/jgrd.50530, 2013.

Hays, M. D., Preston, W., George, B. J., Schmid, J., Baldauf, R., Snow, R., Robinson, J. R., Long, T., and Faircloth, J.: Carbonaceous aerosols emitted from light-duty vehicles operating on gasoline and ethanol fuel blends, Environmental science & technology, 47, 14502-14509, 10.1021/es403096v, 2013.

Hu, W., Hu, M., Hu, W., Jimenez, J. L., Yuan, B., Chen, W., Wang, M., Wu, Y., Chen, C., Wang, Z., Peng, J., Zeng, L., and Shao, M.: Chemical composition, sources, and aging process of submicron aerosols in Beijing: Contrast between summer and winter, Journal of Geophysical Research-Atmospheres, 121, 1955-1977, 10.1002/2015jd024020, 2016.

Huang, R.-J., Zhang, Y., Bozzetti, C., Ho, K.-F., Cao, J.-J., Han, Y., Daellenbach, K. R., Slowik, J. G., Platt, S. M., Canonaco, F., Zotter, P., Wolf, R., Pieber, S. M., Bruns, E. A., Crippa, M., Ciarelli, G., Piazzalunga, A., Schwikowski, M., Abbaszade, G., Schnelle-Kreis, J., Zimmermann, R., An, Z., Szidat, S., Baltensperger, U.,

16

Haddad, I. E., and Prévôt, A. S. H.: High secondary aerosol contribution to particulate pollution during haze events in China, Nature, 10.1038/nature13774, 2014.

Ito, Y., Shimoda, T., Aoki, T., Yuuki, K., Sakamoto, H., Kato, K., Their, D., Kattouah, P., Ohara, E. and Vogt, C.: Next Generation of Ceramic Wall Flow Gasoline Particulate Filter with Integrated Three Way Catalyst, SAE Technical Paper 2015-01-1073, 2015, doi:10.4271/2015-01-1073, 2015.

Jathar, S. H., Gordon, T. D., Hennigan, C. J., Pye, H. O. T., Pouliot, G., Adams, P. J., Donahue, N. M., and Robinson, A. L.: Unspeciated organic emissions from combustion sources and their influence on the secondary organic aerosol budget in the United States, Proc. Natl. Acad. Sci. USA, 111, 10473-10478, 10.1073/pnas.1323740111, 2014.

Jathar, S. H., Woody, M., Pye, H. O. T., Baker, K. R., and Robinson, A. L.: Chemical transport model simulations of organic aerosol in southern California: model evaluation and gasoline and diesel source contributions, Atmospheric Chemistry and Physics, 17, 4305-4318, 10.5194/acp-17-4305-2017, 2017.

Kamal, A., Cincinelli, A., Martellini, T., and Malik, R. N.: A review of PAH exposure from the combustion of biomass fuel and their less surveyed effect on the blood parameters, Environmental Science and Pollution Research, 22, 4076-4098, 10.1007/s11356-014-3748-0, 2015.

Kanakidou, M., Seinfeld, J. H., Pandis, S. N., Barnes, I., Dentener, F. J., Facchini, M. C., Van Dingenen, R., Ervens, B., Nenes, A., Nielsen, C. J., Swietlicki, E., Putaud, J. P., Balkanski, Y., Fuzzi, S., Horth, J., Moortgat, G. K., Winterhalter, R., Myhre, C. E. L., Tsigaridis, K., Vignati, E., Stephanou, E. G., and Wilson, J.: Organic aerosol and global climate modelling: a review, Atmospheric Chemistry and Physics, 5, 1053-1123, 2005.

Kramp, F., and Paulson, S. E.: On the uncertainties in the rate coefficients for OH reactions with hydrocarbons, and the rate coefficients of the 1,3,5-trimethylbenzene and m-xylene reactions with OH radicals in the gas phase, Journal of Physical Chemistry A, 102, 2685-2690, 10.1021/jp973289o, 1998.

Li, M., Hu, M., Wu, Y., Qin, Y., Zheng, R., Peng, J., Guo, Q., Xiao, Y., Hu, W., Zheng, J., Du, Z., Xiao, J., Shuai, S.: Characteristics of Particulate Organic Matters Emissions from Gasoline Direct Injection Engine and Its Influence Factors, Proceedings of the Chinese Society of Electrical Engineering, 36, 4443-4451.

Liang, B., Ge, Y., Tan, J., Han, X., Gao, L., Hao, L., Ye, W., and Dai, P.: Comparison of PM emissions from a gasoline direct injected (GDI) vehicle and a port fuel injected (PFI) vehicle measured by electrical low pressure impactor (ELPI) with two fuels: Gasoline and M15 methanol gasoline, Journal of Aerosol Science, 57, 22-31, 10.1016/j.jaerosci.2012.11.008, 2013.

Lindinger, W., Hansel, A., and Jordan, A.: On-line monitoring of volatile organic compounds at pptv levels by means of proton-transfer-reaction mass spectrometry (PTR-MS) - Medical applications, food control and environmental research, International Journal of Mass Spectrometry, 173, 191-241, 10.1016/s0168-1176(97)00281-4, 1998.

Liu, T., Wang, X., Deng, W., Hu, Q., Ding, X., Zhang, Y., He, Q., Zhang, Z., Lü, S., Bi, X., Chen, J., and Yu, J.: Secondary organic aerosol formation from photochemical aging of light-duty gasoline vehicle exhausts in a smog chamber, Atmos. Chem. Phys. , 15, 9049-9062, 10.5194/acp-15-9049-2015, 2015.

Lu, K. D., Hofzumahaus, A., Holland, F., Bohn, B., Brauers, T., Fuchs, H., Hu, M., Häseler, R., Kita, K., Kondo, Y., Li, X., Lou, S. R., Oebel, A., Shao, M., Zeng, L. M., Wahner, A., Zhu, T., Zhang, Y. H., and Rohrer, F.: Missing OH source in a suburban environment near Beijing: observed and modelled OH and HO_2 concentrations in summer 2006, Atmos. Chem. Phys. , 13, 1057-1080, 10.5194/acp-13-1057-2013, 2013.

Maricq, M. M., Podsiadlik, D. H., and Chase, R. E.: Gasoline vehicle particle size distributions: Comparison of steady state, FTP, and US06 measurements, Environmental science & technology, 33, 2007-2015, 10.1021/es981005n, 1999.

Mathis, U., Mohr, M., and Forss, A. M.: Comprehensive particle characterization of modern gasoline and diesel passenger cars at low ambient temperatures, Atmospheric Environment, 39, 107-117, 10.1016/j.atmosenv.2004.09.029, 2005.

May, A. A., Nguyen, N. T., Presto, A. A., Gordon, T. D., Lipsky, E. M., Karve, M., Gutierrez, A., Robertson, W. H., Zhang, M., Brandow, C., Chang, O., Chen, S., Cicero-Fernandez, P., Dinkins, L., Fuentes, M., Huang, S.-M., Ling, R., Long, J., Maddox, C., Massetti, J., McCauley, E., Miguel, A., Na, K., Ong, R., Pang, Y., Rieger, P., Sax, T., Tin, T., Thu, V., Chattopadhyay, S., Maldonado, H., Maricq, M. M., and Robinson, A. L.: Gas- and particle-phase

444 primary emissions from in-use, on-road gasoline and diesel vehicles, Atmospheric Environment, 88, 247-260,

445 10.1016/j.atmosenv.2014.01.046, 2014.

446 Myung, C.-L., Kim, J., Choi, K., Hwang, I. G., and Park, S.: Comparative study of engine control strategies for

447 particulate emissions from direct injection light-duty vehicle fueled with gasoline and liquid phase liquefied

448 petroleum gas (LPG), Fuel, 94, 348-355, 10.1016/j.fuel.2011.10.041, 2012.

449 Ng, N. L., Kroll, J. H., Chan, A. W. H., Chhabra, P. S., Flagan, R. C., and Seinfeld, J. H.: Secondary organic aerosol

450 formation from m-xylene, toluene, and benzene, Atmos. Chem. Phys. , 7, 3909–3922, 2007.

451 Nordin, E. Z., Eriksson, A. C., Roldin, P., Nilsson, P. T., Carlsson, J. E., Kajos, M. K., Hellén, H., Wittbom, C.,

452 Rissler, J., Löndahl, J., Swietlicki, E., Svenningsson, B., Bohgard, M., Kulmala, M., Hallquist, M., and Pagels, J.

453 H.: Secondary organic aerosol formation from idling gasoline passenger vehicle emissions investigated in a smog

454 chamber, Atmos. Chem. Phys. , 13, 6101-6116, 10.5194/acp-13-6101-2013, 2013.

455 Odum, J. R., Hoffmann, T., Bowman, F., Collins, D., Flagan, R. C., and Seinfeld, J. H.: Gas/particle partitioning

456 and secondary organic aerosol yields, Environ. Sci. Technol., 30, 2580-2585, 10.1021/es950943+, 1996.

457 Peng, J., Hu, M., Du, Z., Wang, Y., Zheng, J., Zhang, W., Yang, Y., Qin, Y., Zheng, R., Xiao, Y., Wu, Y., Lu, S., Wu,

458 Z., Guo, S., Mao, H., and Shuai, S.: Gasoline aromatic: a critical determinant of urban secondary organic aerosol

459 formation, Atmospheric Chemistry and Physics, 2017, in press.

460 Platt, S. M., El Haddad, I., Zardini, A. A., Clairotte, M., Astorga, C., Wolf, R., Slowik, J. G., Temime-Roussel, B.,

461 Marchand, N., Ježek, I., Drinovec, L., Močnik, G., Möhler, O., Richter, R., Barmet, P., Bianchi, F., Baltensperger,

462 U., and Prévôt, A. S. H.: Secondary organic aerosol formation from gasoline vehicle emissions in a new mobile

463 environmental reaction chamber, Atmos. Chem. Phys. , 13, 9141-9158, 10.5194/acp-13-9141-2013, 2013.

464 Robinson, A. L., Donahue, N. M., Shrivastava, M. K., Weitkamp, E. A., Sage, A. M., Grieshop, A. P., Lane, T. E.,

465 Pierce, J. R., and Pandis, S. N.: Rethinking organic aerosols: Semivolatile emissions and photochemical aging,

466 Science, 315, 1259-1262, 10.1126/science.1133061, 2007.

467 Saliba, G., Saleh, R., Zhao, Y., Presto, A. A., Lambe, A. T., Frodin, B., Sardar, S., Maldonado, H., Maddox, C.,

468 May, A. A., Drozd, G. T., Goldstein, A. H., Russell, L. M., Hagen, F., and Robinson, A. L.: Comparison of Gasoline

469   Direct-Injection (GDI) and Port Fuel Injection (PFI) Vehicle Emissions: Emission Certification Standards, Cold-

470   Start, Secondary Organic Aerosol Formation Potential, and Potential Climate Impacts, Environmental science &

471   technology, 51, 6542-6552, 10.1021/acs.est.6b06509, 2017.

472   Schauer, J. J., Kleeman, M. J., Cass, G. R. and Simoneit, B. R. T.: Measurement of Emissions from Air Pollution

473   Sources. 5. C1-C32 Organic Compounds from Gasoline-Powered Motor Vehicles, Environmental science &

474   technology, 36, 1169-1180, 2002.

475   Seinfeld, J. H., Kleindienst, T. E., Edney, E. O., and Cohen, J. B.: Aerosol growth in a steady-state, continuous flow

476   chamber: Application to studies of secondary aerosol formation, Aerosol Science and Technology, 37, 728-734,

477   10.1080/02786820390214954, 2003.

478   Song, C., Na, K. S., and Cocker, D. R.: Impact of the hydrocarbon to NOx ratio on secondary organic aerosol

479   formation, Environ. Sci. Technol., 39, 3143-3149, 10.1021/es0493244, 2005.

480   Ueberall, A., Otte, R., Eilts, P., and Krahl, J.: A literature research about particle emissions from engines with direct

481   gasoline injection and the potential to reduce these emissions, Fuel, 147, 203-207, 10.1016/j.fuel.2015.01.012,

482   2015.

483   Wang, Y., Zheng, R., Qin, Y., Peng, J., Li, M., Lei, J., Wu, Y., Hu, M., and Shuai, S.: The impact of fuel compositions

484   on the particulate emissions of direct injection gasoline engine, Fuel, 166, 543-552, 10.1016/j.fuel.2015.11.019,

485   2016.

486   Wang, Z. B., Hu, M., Wu, Z. J., Yue, D. L., He, L. Y., Huang, X. F., Liu, X. G., and Wiedensohler, A.: Long-term

487   measurements of particle number size distributions and the relationships with air mass history and source

488   apportionment in the summer of Beijing, Atmospheric Chemistry and Physics, 13, 10159-10170, 10.5194/acp-13-

489   10159-2013, 2013.

490   Wen, Y., Wang, Y., Fu, C., Deng, W., Zhan, Z., Tang, Y., Li, X., Ding, H., and Shuai, S.: The Impact of Injector

491   Deposits on Spray and Particulate Emission of Advanced Gasoline Direct Injection Vehicle, SAE Technical Paper,

492   2016-01-2284, 10.4271/2016-01-2284, 2016.

493 Yang, B., Ma, P. K., Shu, J. N., Zhang, P., Huang, J. Y. and Zhang, H. X.: Formation mechanism of secondary

494 organic aerosol from ozonolysis of gasoline vehicle exhaust, Environmental Pollution, 234, 960-968,

495 10.1016/j.envpol.2017.12.048, 2018.

496 Yuan, B., Shao, M., de Gouw, J., Parrish, D. D., Lu, S., Wang, M., Zeng, L., Zhang, Q., Song, Y., Zhang, J., and

497 Hu, M.: Volatile organic compounds (VOCs) in urban air: How chemistry affects the interpretation of positive

498 matrix factorization (PMF) analysis, Journal of Geophysical Research: Atmospheres, 117, n/a-n/a,

499 10.1029/2012jd018236, 2012.

500 Zhang, Q., Jimenez, J. L., Canagaratna, M. R., Allan, J. D., Coe, H., Ulbrich, I., Alfarra, M. R., Takami, A.,

501 Middlebrook, A. M., Sun, Y. L., Dzepina, K., Dunlea, E., Docherty, K., DeCarlo, P. F., Salcedo, D., Onasch, T.,

502 Jayne, J. T., Miyoshi, T., Shimono, A., Hatakeyama, S., Takegawa, N., Kondo, Y., Schneider, J., Drewnick, F.,

503 Borrmann, S., Weimer, S., Demerjian, K., Williams, P., Bower, K., Bahreini, R., Cottrell, L., Griffin, R. J.,

504 Rautiainen, J., Sun, J. Y., Zhang, Y. M., and Worsnop, D. R.: Ubiquity and dominance of oxygenated species in

505 organic aerosols in anthropogenically-influenced Northern Hemisphere midlatitudes, Geophysical Research Letters,

506 34, 10.1029/2007gl029979, 2007.

507 Zhang, X., Cappa, C. D., Jathar, S. H., McVay, R. C., Ensberg, J. J., Kleeman, M. J., and Seinfeld, J. H.: Influence

508 of vapor wall loss in laboratory chambers on yields of secondary organic aerosol, Proc. Natl. Acad. Sci. USA, 111,

509 5802-5807, 10.1073/pnas.1404727111, 2014.

510 Zhao, Y., Nguyen, N. T., Presto, A. A., Hennigan, C. J., May, A. A., and Robinson, A. L.: Intermediate Volatility

511 Organic Compound Emissions from On-Road Gasoline Vehicles and Small Off-Road Gasoline Engines,

512 Environmental science & technology, 50, 4554-4563, 10.1021/acs.est.5b06247, 2016.

513 Zhao, Y., Saleh, R., Saliba, G., Presto, A. A., Gordon, T. D., Drozd, G. T., Goldstein, A. H., Donahue, N. M., and

514 Robinson, A. L.: Reducing secondary organic aerosol formation from gasoline vehicle exhaust, Proceedings of the

515 National Academy of Sciences of the United States of America, 114, 6984-6989, 10.1073/pnas.1620911114, 2017.

516   Zhu, R., Hu, J., Bao, X., He, L., Lai, Y., Zu, L., Li, Y., and Su, S.: Tailpipe emissions from gasoline direct injection

517   (GDI) and port fuel injection (PFI) vehicles at both low and high ambient temperatures, Environmental Pollution,

518   216, 223-234, 10.1016/j.envpol.2016.05.066, 2016.

519   Zimmerman, N., Wang, J. M., Jeong, C.-H., Ramos, M., Hilker, N., Healy, R. M., Sabaliauskas, K., Wallace, J. S.,

520   and Evans, G. J.: Field Measurements of Gasoline Direct Injection Emission Factors: Spatial and Seasonal

521   Variability, Environmental science & technology, 50, 2035-2043, 10.1021/acs.est.5b04444, 2016.

522

523 Table 1 Descriptions of the gasoline direct injection (GDI) and port fuel injection (PFI) vehicles used in the

524 experiments.

Vehicle	Make and model	Emission standard class	Model year	Mileage (km)	Displacement (cm^3)	Power (kW)	Weight (kg)
GDI	VW Sagitar	China V	2015	3000	1395	110	1395
PFI	Honda Civic	China IV	2009	42500	1799	103	1280

525

526 Table 2 Overview of all instruments used to measure the gas and particulate phase pollutants in the experiments.

Parameter	Phase	Instrument	Note
CO, CO_2, NO_x and total hydrocarbon (THC) concentration	Gas	Gas analyzer AVL Combustion Emissions Bench II	On-line
Aerosol number size distribution	Particle	DMS500	On-line
$PM_{2.5}$	Particle	Balance (AX105DR)	Off-line
Organic carbon/Elemental carbon concentration	Particle	OC/EC analyzer	Off-line
CO concentration	Gas	48i CO analyzer	On-line
NO, NO_2, and NO_x concentration	Gas	42i NO-NO_2-NO_x analyzer	On-line
O_3 concentration	Gas	49i O_3 analyzer	On-line
VOCs concentration	Gas	Proton transfer reaction mass spectrometer (PTR-MS)	On-line
Aerosol number (mass) size distribution	Particle	Scanning mobility particle sizer (SMPS, consist of 3081-DMA and 3775-CPC),	On-line
Size resolved non-refractory aerosol	Particle	High resolution time-of-flight aerosol mass spectrometer (HR-Tof-AMS)	On-line

527

528

529   Table 3 Emission factors (EFs) of gaseous pollutants from the gasoline direct injection (GDI) and port fuel injection (PFI) vehicles in

530   this study and those of previous studies.

	This study				Saliba et al., 2017		May et al., 2014	Platt et al., 2013		Zhu et al., 2016	
	GDI		PFI		GDI	PFI	PFI[a]			GDI	PFI
	China V		China IV		ULEV	ULEV	LEV II	Euro V		China IV	China IV
	Cold BJC				Cold UC[b]		Cold UC	Cold NEDC		Cold WLTC[c]	
	g kg-fuel^{-1}	g km^{-1}	g kg-fuel^{-1}	g km^{-1}	g km^{-1}	g km^{-1}	g kg-fuel^{-1}	g kg-fuel^{-1}	g km^{-1}	g km^{-1}	g km^{-1}
CO_2	3439 ±23	213 ±4	3350 ±24	283 ±4	-	-	-	-	-	187	215
THC	1.55 ±0.22	0.09 ±0.01	1.70 ±0.19	0.13 ±0.01	0.02	0.06	0.64	0.91-1.06	0.036-0.042	0.05	0.03
Benzene	0.056 ±0.011	0.003 ±0.001	0.061 ±0.016	0.005 ±0.001	-	-	0.018	-	0.002	-	-
Toluene	0.101 ±0.004	0.006 ±0.001	0.220 ±0.047	0.017 ±0.004	-	-	0.026	-	0.002	-	-

531   [a] 22 PFI vehicles and 3 GDI vehicles;

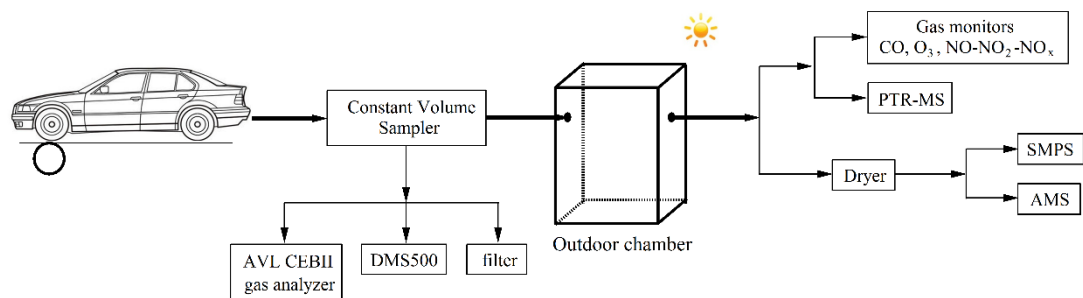532   [b] UC: Unified Cycle;

533   [c] WLTC: Worldwide-harmonized Light-duty Test Cycle

534   Table 4 EFs of primary aerosols, including carbonaceous aerosols and particulate polycyclic aromatic hydrocarbons (PAHs) from the

535   GDI and PFI vehicles in this study and those of previous studies.

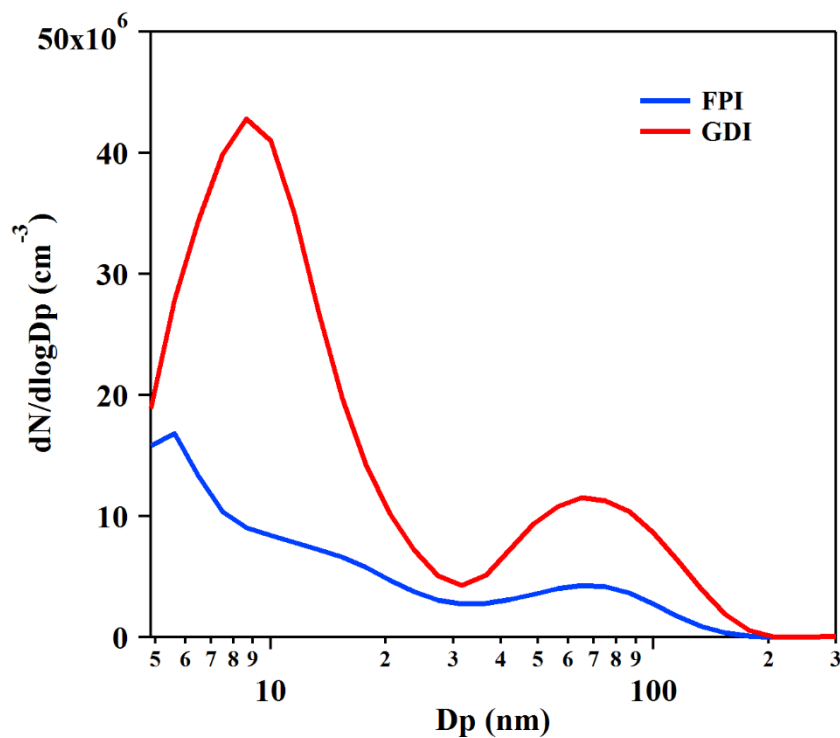|	This study				Saliba et al., 2017		May et al., 2014	Platt et al., 2013		Zhu et al., 2016	
	GDI		PFI		GDI	PFI	PFI			GDI	PFI
	China V		China IV		ULEV	ULEV	LEV II	Euro V		China IV	China IV
	Cold BJC				Cold UC		Cold UC	Cold NEDC		Cold WLTC	
	mg kg-fuel⁻¹	mg km⁻¹	mg kg-fuel⁻¹	mg km⁻¹	mg km⁻¹	mg km⁻¹	mg kg-fuel⁻¹	mg kg-fuel⁻¹	mg km⁻¹	mg km⁻¹	mg km⁻¹
PM$_{2.5}$	61.7±24.5	3.4±1.4	33.4±25.6	2.5±1.9	3.9	2.4	18.0	-	-	1.5	1.0
EC	10.7±3.6	0.6±0.2	2.4±1.6	0.2±0.1	3.0	0.6	12.2	11.2-20.0	1.2-1.7	-	-
POA	41.7±9.8	2.3±0.6	25.0±0.3	1.9±0.1	0.4	0.6	5.2	24.5-19.7	0.4-1.4	-	-
OC/EC	3.2		8.7		0.1	0.8	0.4	0.2-1.8		-	-
PAHs(×10⁶)	20.4±2.1	1.1±0.1	13.2±4.1	1.0±0.3	-	-	-	-	-	-	-

536

537

26

538

539   Figure 1. Schematic diagram of the outdoor chamber set up for the experiments.

540

Figure 2. Number size distributions of primary PM emitted from the GDI (red line) and PFI (blue line) gasoline vehicles. The results are average of particle number emissions from vehicles during a whole BJC, measured by DMS500 in the CVS system. The particles were heated to 150℃ in the DMS500.
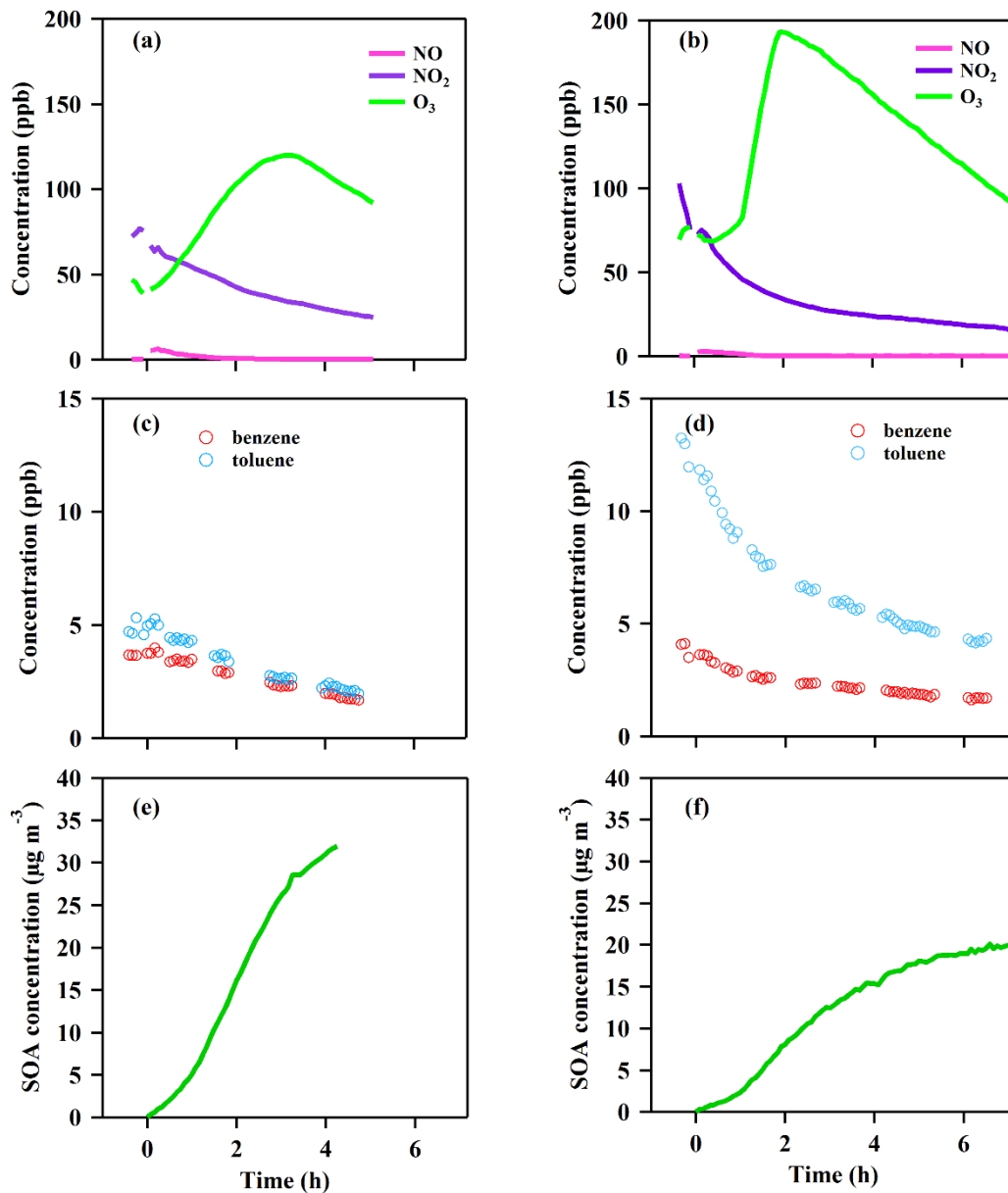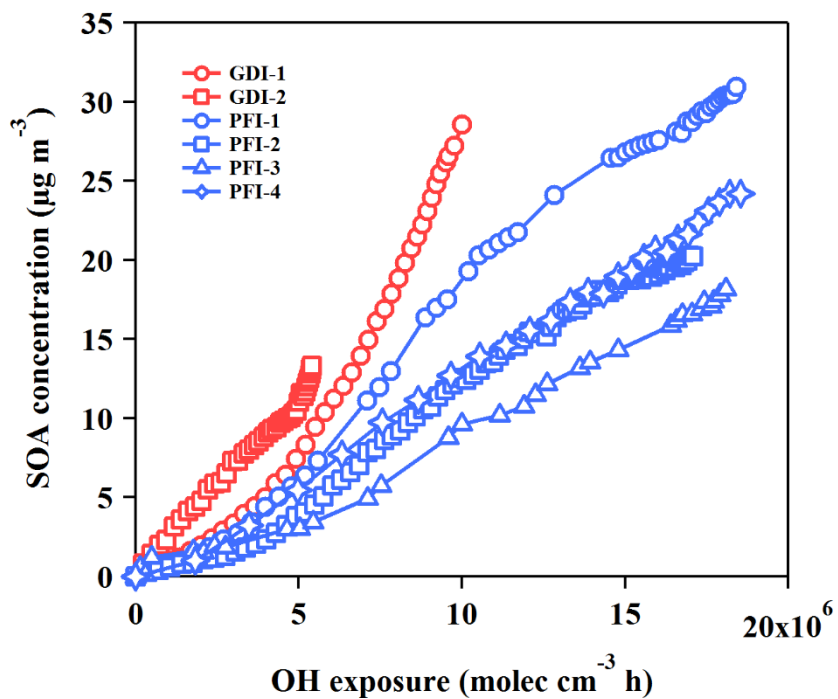
546

Figure 3. Time series of the gases and particle evolutions over the photochemical age in the chamber experiments

from the GDI vehicle exhaust (a, c, e) and PFI vehicle exhaust (b, d, f). (a, b): NO, NO_2 and O_3 concentration; (c,

d): benzene and toluene concentration; (e, f): corrected SOA concentration.

550

551

Figure 4. SOA productions from the GDI vehicle exhaust (red markers) and the PFI vehicle exhaust (blue markers)

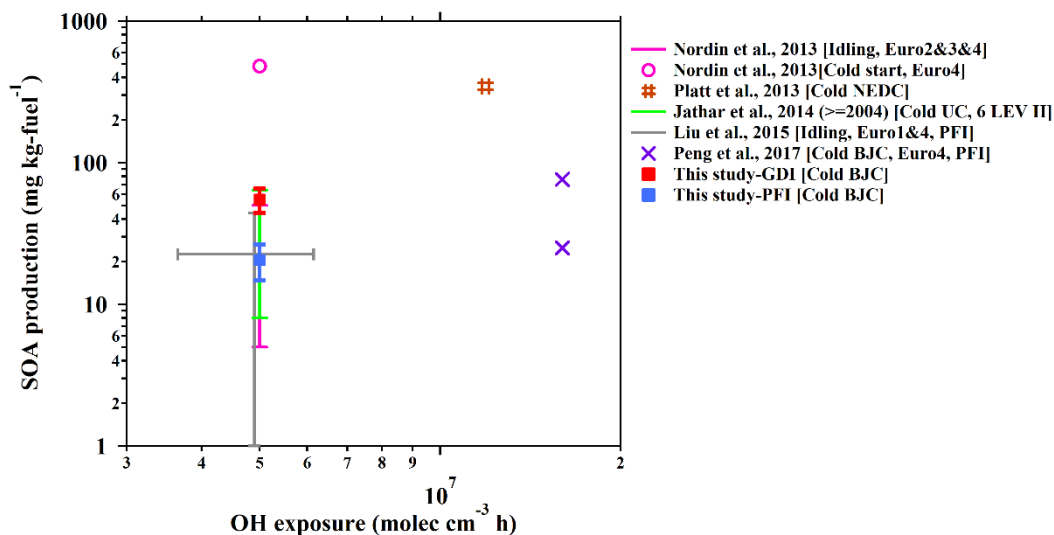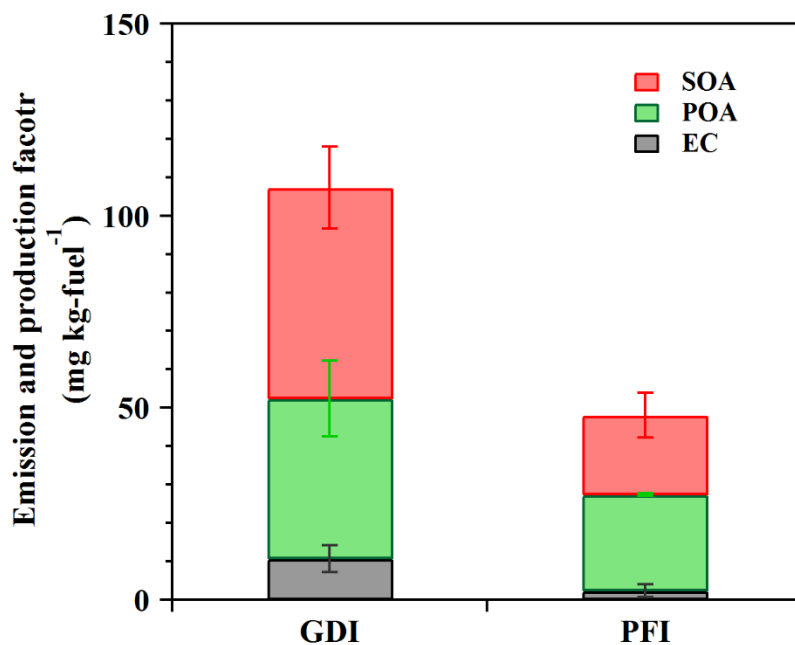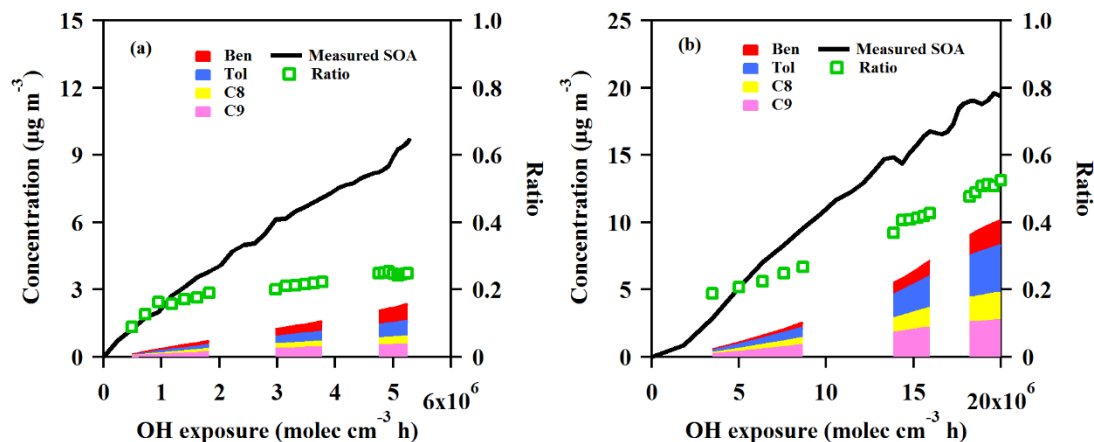553 as functions of OH exposure in the chamber experiments.

554

Figure 5. Fuel-based SOA production from gasoline vehicle exhaust as a function of OH exposure in the chamber simulations. The SOA production data are from published studies of chamber simulation of gasoline vehicle exhaust. From the study of Jathar et al. (2014), the SOA production of vehicles manufactured in 2004 or later (LEV II) is selected, which is a model year that is more close to those of the vehicles in this study. The error bars of previous results indicate the range of OH exposure (x axis) and SOA production (y axis) in their simulations. The driving cycles and vehicle information are also noted in the legend of each study.

Figure 6 EC and POA EFs as well as corrected SOA production factors from the GDI and PFI vehicle exhausts in this study (OH exposure = 5×10^6 molecular cm^{-3} h).

567

568 Figure 7. Measured and predicted SOA concentration as a function of OH exposure from GDI vehicle exhaust (a)

569 and PFI vehicle exhaust (b) in the chamber experiments. The black line is the measured SOA concentration with

570 wall-loss and particle dilution correction during the experiment. The red, blue, yellow and pink areas are predicted

571 SOA concentration estimated from benzene, toluene, C8 benzene and C9 benzene, respectively. The green markers

572 are the ratios of the predicted SOA to the measured SOA.

573

1 **Supplementary information**

2 **Comparison of primary aerosol emission and secondary aerosol formation from gasoline**

3 **direct injection and port fuel injection vehicles**

4 Zhuofei Du[1], Min Hu[1, 3*], Jianfei Peng[1†], Wenbin Zhang[2], Jing Zheng[1], Fangting Gu[1], Yanhong

5 Qin[1], Yudong Yang[1], Mengren Li[1], Yusheng Wu[1], Min Shao[1], Shijin Shuai[2]

6 1. State Key Joint Laboratory of Environmental Simulation and Pollution Control, College of

7   Environmental Sciences and Engineering, Peking University, Beijing 100871, China

8 2. State Key Laboratory of Automotive Safety and Energy, Department of Automotive

9   Engineering, Tsinghua University, Beijing 100084, China

10 3. Beijing Innovation Center for Engineering Sciences and Advanced Technology, Peking

11   University, Beijing 100871, China

12 [†] Now at Department of Atmospheric Sciences, Texas A&M University, College Station, TX

13   77843, US

14

15 *Corresponding author: Min Hu, minhu@pku.edu.cn

16

Data correction

Wall-loss correction as well as particle and gas dilution corrections were considered in this study. The details of wall-loss correction are introduced by Du et al. (2017). The real-time instruments sampled from the chamber during the whole photo-oxidation experiment, and zero air was added to maintain a constant pressure inside the chamber. This led to particle dilution that the sampled particles would not be included in the subsequent measurement, and gas dilution that the sampled gas would not participate in the subsequent photo-oxidation reaction and SOA formation. The particle dilution corrected mass concentration $C_{corr,n+1}$ could be calculated as:

$$C_{corr,n+1} = C_{n+1} + \sum_{i=1}^{n}(k_{wall} \times C_i) + \sum_{i=1}^{n}(k_{dilu,i} \times C_i) \tag{1}$$
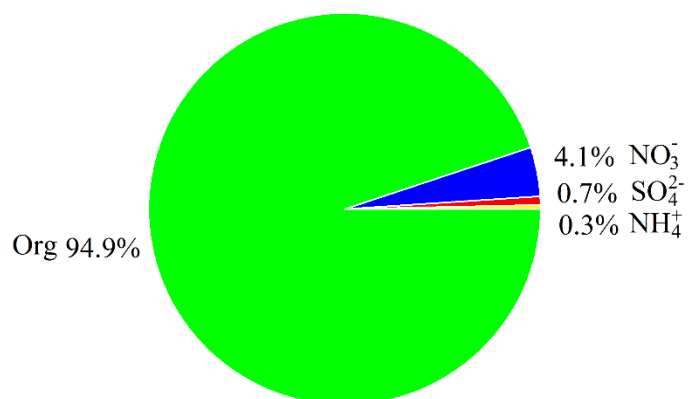
where C_{n+1} was the measured particle mass concentration at time n+1, k_{wall} was the wall loss decay constant and $k_{dilu,i}$ was dilution ratio at time i.

Then the gas dilution was taken into consideration. The final particle mass concentration $C_{final,n+1}$ could be calculated as:

$$C_{final,n+1} = C_{corr,n+1} - C_1 + \sum_{i=1}^{n}\left(\sum_{i=1}^{n+1} k_{dilu,i}\right) \times (C_{corr,n+1} - C_{corr,n}) \tag{2}$$

References

Du, Z., Hu, M., Peng, J., Guo, S., Zheng, R., Zheng, J., Shang, D., Qin, Y., Niu, H., Li, M., Yang, Y., Lu, S., Wu, Y., Shao, M., and Shuai, S.: Potential of secondary aerosol formation from Chinese gasoline engine exhaust, Journal of environmental sciences, in press.

40

4.1% NO_3^-
0.7% SO_4^{2-}
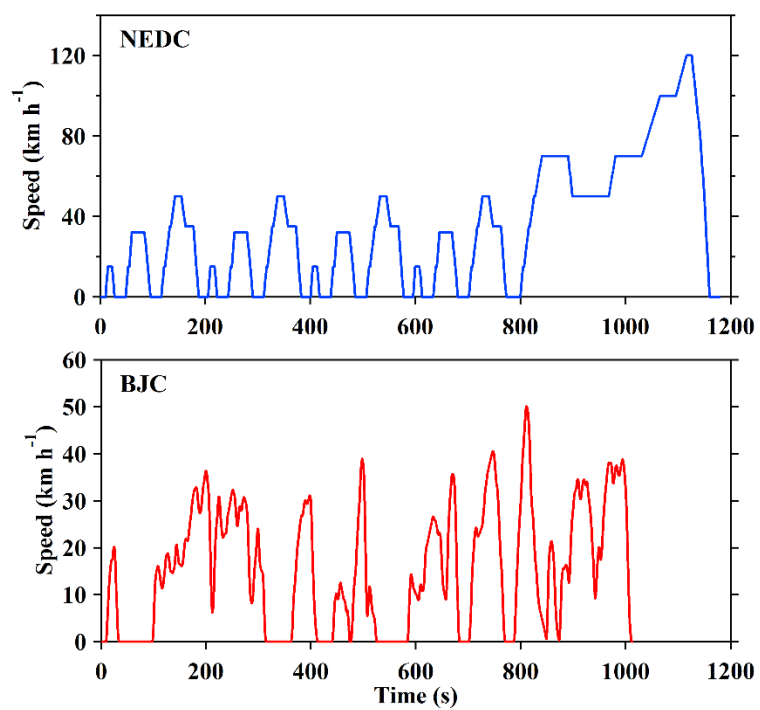0.3% NH_4^+
Org 94.9%

41

42 Figure S1. Chemical composition of secondary aerosol formed in the chamber experiment

43 (Experiment GDI-1).

44

45

46

47   Figure S2. Speed profiles of NEDC and BJC driving cycle.

48

49   Table S1 Details of the fuel used in the experiments.

Specifications	Fuel
Density (g mL^{-1})	0.7
Rvp (kPa)	55.4
Aromatics (% v/v)	36.7
Olefin (% v/v)	15.4
Ethanol (% v/v)	0.01
Oxygen (% m/m)	0.02
Mn (mg kg^{-1})	< 0.1
Sulfur (mg kg^{-1})	6
T10 (℃)	55.4
T50 (℃)	109.9
T90 (℃)	164.3
Fbp (℃)	194.4

50

51

Table S2 The EFs of Particulate-phase PAHs from GDI and PFI vehicles.

Compound	Emission factor (ng kg-fuel^{-1})	
	GDI	PFI
Napthalene	0.025	<0.0001
1-Methylnaphthalene	<0.0001	<0.0001
2-Methylnaphthalene	0.012	0.004
2,6-Dimethylnaphthalene	0.006	0.003
Acenaphthylene	0.012	0.009
Acenapthene	<0.0001	0.015
Fluorene	0.003	0.105
Methyl-fluorene	0.083	0.105
Dibenzofuran	0.006	0.039
Retene	0.009	0.011
9-Methylanthracene	<0.0001	0.013
Phenanthrene	0.244	0.069
Anthracene	0.048	0.018
Fluoranthene	0.201	0.034
Pyrene	0.246	0.029
Methyl-fluoranthene	0.004	0.007
Benzo[a]anthracene	0.006	0.036
Chrysene	0.020	0.065
Methyl-chrysene	<0.0001	0.007
Benzo[b]fluoranthene	0.034	0.147
Benzo[k]fluoranthene	0.041	0.129
Benzo[e]pyrene	0.028	0.051
Benzo[a]pyrene	0.012	0.041
Benzo[ghi]flouranthene	0.095	0.027
Cyclopenta[cd]pyrene	<0.0001	0.032
Dibenzo[a,h]anthracene	<0.0001	<0.0001

Picene	<0.0001	<0.0001
Perylene	0.009	<0.0001
Benzo[ghi]perylene	<0.0001	<0.0001
Indeno[1,2,3-cd]pyrene	<0.0001	<0.0001
Coronene	<0.0001	<0.0001
Sum PAHs	1.144	0.994

53